RAYRA DESTRO

Identification and predictive control applied to a quadruple tank

São Paulo
2023

RAYRA DESTRO

Identification and predictive control applied to a quadruple tank

Corrected Version

Thesis submitted to Escola Politécnica of the Universidade de São Paulo for degree of Master of Science.

São Paulo
2023

RAYRA DESTRO

Identification and predictive control applied to a quadruple tank

Corrected Version

Thesis submitted to Escola Politécnica of the Universidade de São Paulo for degree of Master of Science.

Concentration area:

3139 - Systems Engineering

Advisor:

Prof. Dr. Claudio Garcia

São Paulo
2023

Este exemplar foi revisado e corrigido em relação à versão original, sob responsabilidade única do autor e com a anuência de seu orientador.

São Paulo, _____ de _____ de _____

Assinatura do autor: _____

Assinatura do orientador: _____

Catalogação-na-publicação

Destro, Rayra
Identification and predictive control applied to a quadruple tank / R. Destro -- versão corr. -- São Paulo, 2023.
64 p.

Dissertação (Mestrado) - Escola Politécnica da Universidade de São Paulo. Departamento de Engenharia de Telecomunicações e Controle.

1.Quadruple Tank 2.System Identification 3.MPC 4.Predictive Control I.Universidade de São Paulo. Escola Politécnica. Departamento de Engenharia de Telecomunicações e Controle II.t.

RESUMO

Este trabalho foca na identificação de um sistema de tanque quádruplo e em seu controle, utilizando técnicas de controle preditivo. É descrita a construção da planta com tanques quádruplos e feita a sua modelagem fenomenológica. Também são descritas técnicas de identificação de sistemas e seus testes para o conjunto de tanques. São descritas as técnicas de controle MPC, IHMPC e ESC e com estas técnicas são realizados teste comparativos com a planta identificada em questão. Por fim, são apresentados os resultados e as conclusões.

Palavras-Chave – Tanque Quádruplo, Identificação de Sistemas, MPC, controle preditivo.

ABSTRACT

This work focuses on system identification of a quadruple tank and on its control using predictive control techniques. The construction of the plant is detailed and its phenomenological model is designed. System identification techniques are described and the validation tests are shown. MPC, IHMP and ESC techniques are presented as well as their comparison tests considering the identified plant. Results and conclusions are presented at the end.

Keywords – Quadruple Tank, System Identification, MPC, Predictive Control.

LIST OF FIGURES

CONTENTS

1 INTRODUCTION

Modeling and controlling plants are usual activities in the industrial environment. Even though these activities are common in the industry, they are not trivial. Phenomenological modeling has an issue: gathering all system parameters and their peculiarities. To avoid such difficulties, techniques such as system identification are quite useful in this situation.

As the quadruple tank is a well-known system, the meaning of using identification, in this case, is to study and compare the results of different identification models with the phenomenological model that is designed. The system is MIMO like most industrial plants. Besides being a non-linear plant, it has an adjustable zero which can be of minimum phase or non-minimum phase (JOHANSSON, 2000).

System identification is a modeling technique that consists on collecting inputs and outputs of the system subject to known conditions. Based on the information that can be obtained from them, a polynomial model is written (LJUNG, 1999). The PRBS signal is a known input which is commonly used for identification. Due to its composition it is able to provide the necessary information of the plant when correctly used (AGUIRRE, 2015).

There are plenty different structures used in system identification. In this work the structures ARX, ARMAX, OE and BJ are used.

There are a lot of publications exploring different controls for the quadruple tank such as H_{inf} (LI; ZHENG, 2014) and decoupled PID (ASTROM; JOHANSSON; WANG, 2002), for example. The practical quadruple tank in Escola Politécnica of USP, which is used in this work was also used to explore discrete LQG/LTR (NEVES et al., 2016) controls and QFT with dynamic decoupling (NEVES; ANGÉLICO, 2016).

The Model Predictive Control (MPC) is the control technique focused on this work. MPC predicts the future response of a plant based on an explicit process model. This control was originally designed to meet specific needs of oil refineries and now can be

found in different kinds of plants (QIN; BADGWELL, 2003).

The MPC calculates a series of admissible control inputs capable of taking the system to a certain point. For that, it is necessary to satisfy some restrictions and to minimize a cost function (FERRAMOSCA et al., 2009).

Similarly, IHMPC generates control inputs based on prediction but considering an infinity horizon. Caused by this specificity, for the implementation, it was considered the necessity of remodeling the system using OPOM (MARTINS M. A.; ODLOAK, 2016). The technique has lots of variations but at this work there will be explored only a simpler implementation.

In addition to these predictive controllers, it was chosen to use as comparison a model-free control technique (DESTRO et al., 2021). The main purpose was to use a straightforward methodology, that considers only the calculus of inputs based on the outputs to converge the an optimum point.

This work contemplates the developed activities in five more chapters. Firstly, in Chapter 2 the phenomenological model is designed. In Chapter 3 the identification techniques used in this work are explored. Next, the MPC, IHMPC and ESC controllers are designed in Chapter 4. Chapter 5 shows the results obtained. And lastly, the conclusions are shown in Chapter 6.

2 MODELING

In this chapter, it is developed the phenomenological model for the quadruple tank system. In addition to that, the identification of the plant is perfirmed.

2.1 General overlook

The quadruple tank system is composed of four main tanks, a reservoir, two pumps and two proportional valves (ASTROM; JOHANSSON; WANG, 2002). The tanks are connected as shown in Figure 1.

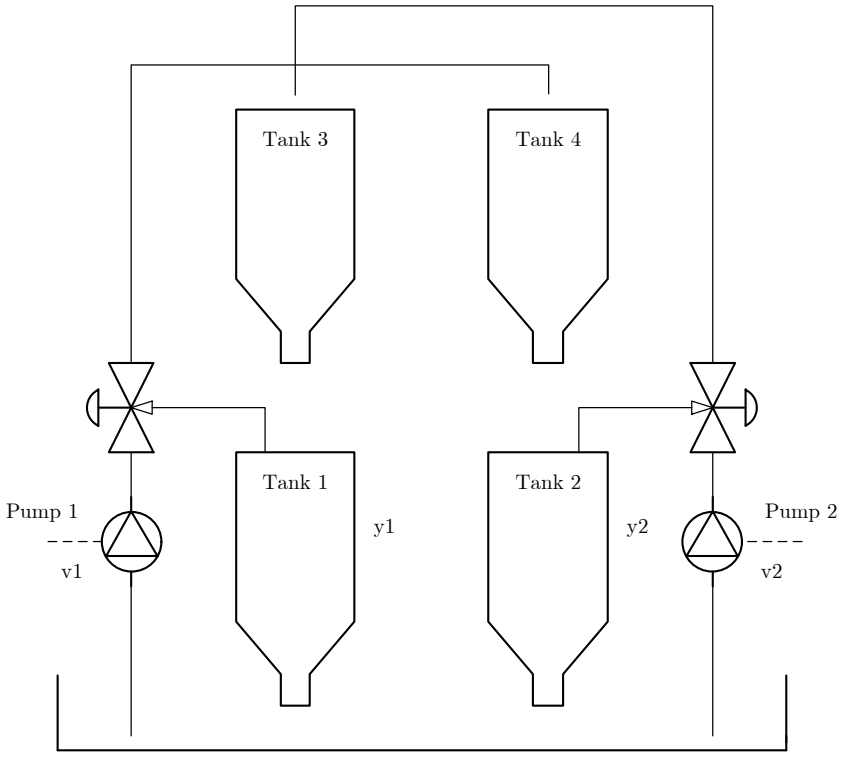

Figure 1: Quadruple tank.

Pump 1 is responsible for pumping water from the reservoir to tank 1 and to tank 4 and the proportion of water is based on valve 1 opening. Similarly, pump 2 supplies

water to tank 2 and tank 3. In this case, the proportion is given by valve 2. So tank 3 supplies water for tank 1 and tank 4 supplies water to tank 2. Tank 1 and tank 2 return the water to the reservoir.

2.2 Phenomenological model

The main problem to be solved is to control the liquid level in tanks 1 and 2, using only the supply voltage of both pumps. The mass balance of the system is considered for modeling it. Turbulent regime is assumed. Tank 1: it has an input that brings in the fluid from tank 3 by gravity and another one which is provided by the pump 1 combined with valve 1. Its output is the leaking fluid to the reservoir by gravity. Applying this concept for all the tanks, the dynamic equations are obtained as:

$$\frac{dh_1}{dt} = -\frac{a_1}{A_1}\sqrt{2gh_1} + \frac{a_3}{A_1}\sqrt{2gh_3} + \frac{\gamma_1 k_1 v_1}{A_1} \tag{2.1}$$

$$\frac{dh_2}{dt} = -\frac{a_2}{A_2}\sqrt{2gh_2} + \frac{a_4}{A_2}\sqrt{2gh_4} + \frac{\gamma_2 k_2 v_2}{A_2} \tag{2.2}$$

$$\frac{dh_3}{dt} = -\frac{a_3}{A_3}\sqrt{2gh_3} + \frac{(1-\gamma_2) k_2 v_2}{A_3} \tag{2.3}$$

$$\frac{dh_4}{dt} = -\frac{a_4}{A_4}\sqrt{2gh_4} + \frac{(1-\gamma_1) k_1 v_1}{A_4} \tag{2.4}$$

where:

- h_i level of tank i;
- a_i area of liquid exit of tank i;
- A_i area of the base of tank i;
- v_i supply voltage of pump i;
- g gravity acceleration;
- γ_i opening percentage of valve i.

The valve opening is considered as fixed. It determines if the zero of the system is minimum or non-minimum phase (ASTROM; JOHANSSON; WANG, 2002). If:

$$0 < \gamma_1 + \gamma_2 < 1, \tag{2.5}$$

the input-output system presents a non-minimum phase zero. If

$$1 < \gamma_1 + \gamma_2 < 2, \tag{2.6}$$

the input-output system presents a minimum phase zero.

The quadruple tank built is shown in Figure 2.

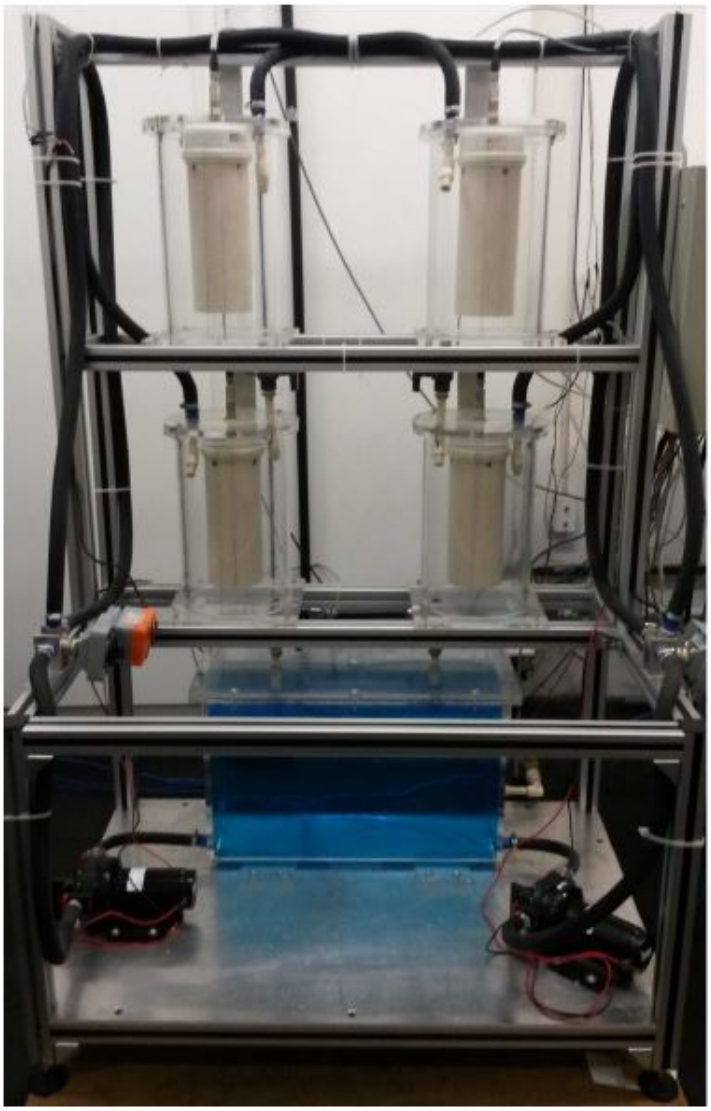

Figure 2: Quadruple tank.

In this case, the parameters are:

- $a_1 = a_2 = 0.4657$ [cm^2];
- $a_3 = a_4 = 0.3421$ [cm^2];
- $A_1 = A_2 = A_3 = A_4 = 254.4690$ [cm^2];
- $k_1 = k_2 = 18$ [cm^3/(V*s)];
- $\gamma_1 = 0.55$;
- $\gamma_2 = 0.54$.

- u is the voltage applied to the pump, ranging from 0V to 10V.

As in this work it is going to be used a linear control, it is necessary to obtain a linear model around operating points. It is assumed that the operating point, in this case, are $\bar{h}_1 = 15$cm and $\bar{h}_2 = 15$cm and they are fixed. Assuming that

$$x_i = h_i - \bar{h}_i \tag{2.7}$$

are system states and

$$u_i = v_i - \bar{v}_i \tag{2.8}$$

are the entrances of the state space model (JOHANSSON, 2000), which is written as:

$$\dot{x} = \begin{bmatrix} -\frac{1}{T_1} & 0 & \frac{A_3}{A_1 T_3} & 0 \\ 0 & -\frac{1}{T_2} & 0 & \frac{A_4}{A_2 T_2} \\ 0 & 0 & -\frac{1}{T_3} & 0 \\ 0 & 0 & 0 & -\frac{1}{T_4} \end{bmatrix} x + \begin{bmatrix} \frac{\gamma_1 k_1}{A_1} & 0 \\ 0 & \frac{\gamma_2 k_2}{A_2} \\ 0 & \frac{(1-\gamma_2) k_2}{A_3} \\ \frac{(1-\gamma_1) k_1}{A_4} & 0 \end{bmatrix} u \tag{2.9}$$

$$y = \begin{bmatrix} 1 & 0 & 0 & 0 \\ 0 & 1 & 0 & 0 \end{bmatrix} x, \tag{2.10}$$

with:

$$T_i = \frac{A_i}{a_i} \sqrt{\frac{2h_i}{g}}. \tag{2.11}$$

Substituting the numerical values and using the sample time $T_s = 1$s, the discrete linear model is given by

$$\begin{aligned} x(k+1) &= A_m x(k) + B_m u(k) \\ y(k) &= C_m x(k) \end{aligned} \tag{2.12}$$

and applying the numerical values it is written as follows:

$$A_m = \begin{bmatrix} 0.9896 & 0 & 0.0207 & 0 \\ 0 & 0.9896 & 0 & 0.0207 \\ 0 & 0 & 0.9792 & 0 \\ 0 & 0 & 0 & 0.9792 \end{bmatrix}. \tag{2.13}$$

$$B_m = \begin{bmatrix} 0.0387 & 0.0003 \\ 0.0003 & 0.0380 \\ 0 & 0.0322 \\ 0.0315 & 0 \end{bmatrix} \tag{2.14}$$

$$C_m = \begin{bmatrix} 1 & 0 & 0 & 0 \\ 0 & 1 & 0 & 0 \end{bmatrix}. \tag{2.15}$$

This model is going to be used as a comparison with the identified model.

2.3 Changes in the plant and impacts to this work

During the process of development of this project, we faced several issues with the practical plant, but some of them changed the course of the work. First, other users of the plant identified that the valves were not able to maintain a constant opening according to the input voltage. Considering investment and use of the plant, the chosen solution was to take the valves out, aware that the plant had changed. With that said, the described phenomenological model is not totally coherent with the plant anymore but still is the source for comparisons for the identified model that is going to be developed next.

The second point is that the LabView in which the project was developed, requires a specific license to work properly and it was not compatible with our firewall so it is not possible to keep working with the software immediately. Considering the deadline for this work, we decided to change the scope of it to use the practical tank until the point of getting data for the identification process. The control part used the best-identified model to be tested and, unfortunately, it was not implemented in the tank but this is clearly the next step for a future job.

3 IDENTIFICATION

In this chapter, it is shown how identification techniques were used in this project. System identification is commonly used for complex systems, where it is hard to model the plant phenomenologically. As the quadruple tank is a well-known system, the intention of using this technique it to study the methodology and to compare its results with the phenomenological model.

3.1 PRBS

As the pseudo-random binary sequence (PRBS) is a signal which is statistically similar to a white noise signal, it was chosen as the input signal for the identification of the system (LJUNG, 1999). Because of that characteristic, this signal is capable of bringing to light relevant behaviors of the system, making the identification methodology possible.

The sampling time chosen is $T_s = 2$s, which is lower than the fastest time constant of the system, and the final decision for this number was made empirically on the plant. During the tests to choose the PRBS features some step signals with a variety of voltages were tested and the value of $u_1 = u_2 = 6$V was considered as one that best fits the need of having a reasonable level for the tanks. Figure 3 shows the tank levels with these values of inputs in the practical plant. The excursion chosen was 0.5V, because it shows a good signal-to-noise ratio and does not make the liquid level too low or too high.

Next, in Figure 4 it is possible to check the PRBS signal used in the identification. Note that we have different signals, one for each input channel, based on the same parameters, but with different seeds.

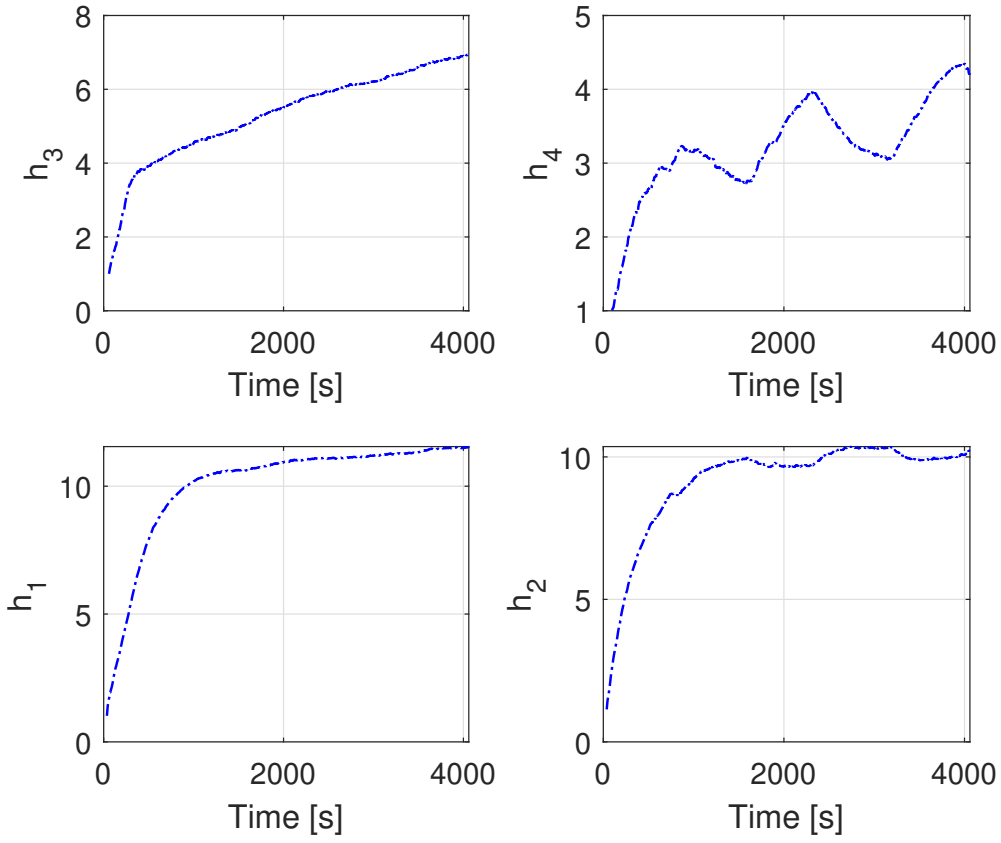

Figure 3: Equilibrium points for tank levels.

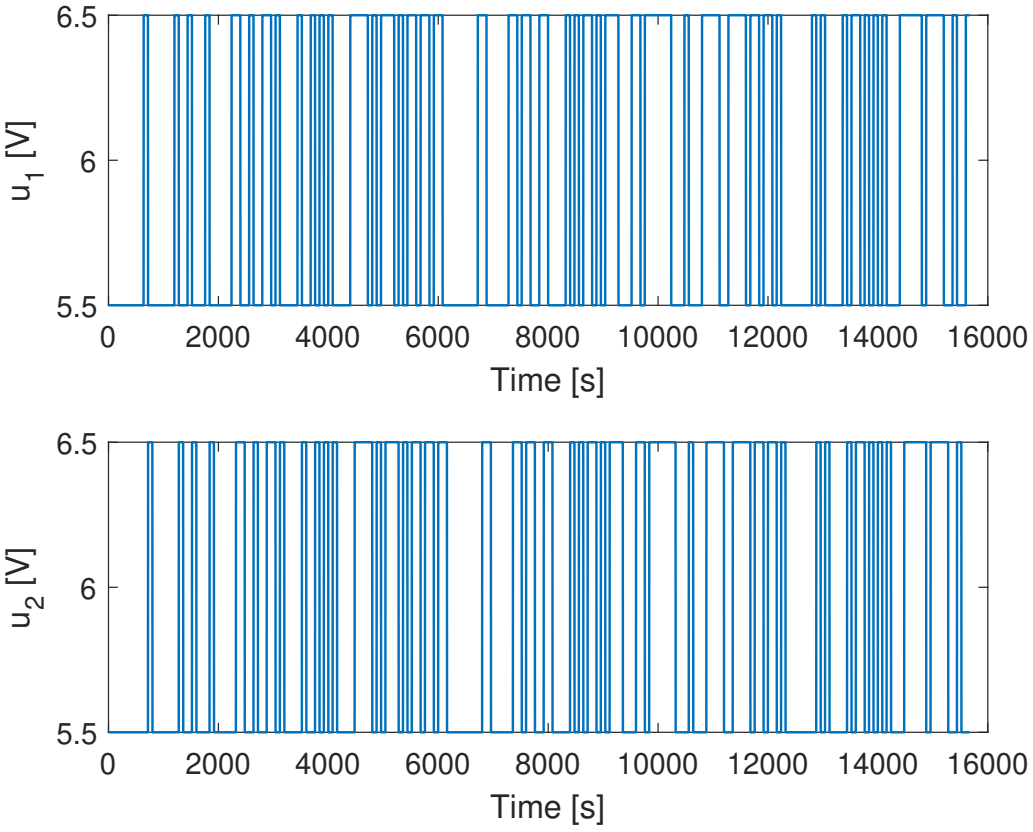

Figure 4: PRBS for both inputs.

3.2 Identified Models

As one of the intentions of this project is to talk about identification models, this work is going to present the following models in a general view: ARX, ARMAX, OE and BJ.

In this chapter, it is going to be used the variable q as is the delay operator. $e(t)$ is the white-noise disturbance value.

3.2.1 ARX

The autoregressive with exogenous input (ARX) model structure is written as follows:

$$A(q)y(t) = B(q)u(t - n_k) + e(t) \tag{3.1}$$

contraction of:

$$\begin{aligned} y(t) + A_1 y(t-1) + A_2 y(t-2) + ... + A_{na} y(t - na) = \\ B_1 u(t - \Delta k) + ... + B_{nb} u(t - nb - nk + 1) + e(t) \end{aligned} \tag{3.2}$$

where:

- n_a - number of poles with one row for each output signal;
- n_b - number of zeros with one row for each output signal;
- n_k - dead time: number of input samples before the output is affected by the input;
- A and B - polynomials in q.

3.2.2 ARMAX

The autoregressive moving average with exogenous input (ARMAX) model structure is written as follows:

$$A(q)y(t) = B(q)u(t - n_k) + C(q)e(t) \tag{3.3}$$

contraction of:

$$\begin{aligned} y(t) + A_1 y(t-1) + A_2 t(t-2) + ... + A_{n_a} y(t - n_a) = B_1 u(t - n_k) + ... + \\ B_{n_b} u(t - n_b - n_k) + C_1 e(t-1) + ... + C_{nc} e(t - n_c) + e(t) \end{aligned} \tag{3.4}$$

where:

- n_a - number of poles with one row for each output signal;
- n_b - number of zeros with one row for each output signal;
- n_c - number of coefficients of polynomial C;
- n_k - dead time: number of input samples before the output is affected by the input;
- A, B and C - polynomials in q.

3.2.3 BJ

The Box-Jenkins (BJ) polynomial model structure is written as follows:

$$y(t) = \sum_{i=1}^{n_u} \frac{B_i(q)}{F_i(q)} u_i(t - n_k i) + \frac{C(q)}{D(q)} e(t) \tag{3.5}$$

with:

$$B(q) = B_1 q^{-n_k} + \cdots + B_{n_b} q^{-n_b - n_k + 1} \tag{3.6}$$

$$C(q) = 1 + C_1 q^{-1} + \cdots + C_{n_c} q^{-n_c} \tag{3.7}$$

$$D(q) = 1 + D_1 q^{-1} + \cdots + D_{n_d} q^{-n_d} \tag{3.8}$$

$$F(q) = 1 + F_1 q^{-1} + \cdots + F_{n_f} q^{-n_f} \tag{3.9}$$

where

- n_b - number of zeros plus 1 with one row for each output signal;
- n_c - number of coefficients of polynomial C;
- n_d - number of coefficients of polynomial D;
- n_f - number of coefficients of polynomial F;
- n_k - dead time: number of input samples before the output is affected by the input;
- n_u - number of input channels;
- B, C, D and F - polynomials in q.

3.2.4 OE

The Output-Error (OE) polynomial model structure is written as follows:

$$y(t) = \frac{B(q)}{F(q)}u(t - n_k) + e(t) \tag{3.10}$$

where:

- n_b - number of zeros plus 1 with one row for each output signal;
- n_f - number of coefficients of polynomial F;
- n_k - dead time: number of input samples before the output is affected by the input;
- n_u - number of input channels;
- B and F - polynomials in q.

3.3 Practical application

An important information on this point is to tell that during the development of this work, the practical plant faced some technical issues and because of that the valves were removed. That said, it is simple to tell that the identification model is not going to be so similar to the phenomenological model showed in previous sections.

4 CONTROLLER

This chapter presents the design for three different controllers. The first section develops the Model Predictive Control, the second goes through the design of Infinite Horizon Model Predictive Control and finally the Extremum Seeking Control is tested and the direct control method presented.

4.1 Model Predictive Control

In this section, the predictive control MPC for the quadruple tank is going to be designed. The state space in incremental form shown next is going to be used in this work.

$$\begin{aligned} x(k+1) &= Ax(k) + B\Delta u(k) \\ y(k) &= Cx(k) \end{aligned} \tag{4.1}$$

where:

$$\Delta u(k) = u(k) - u(k-1). \tag{4.2}$$

The MPC controller is based on predictions of a dynamic model representing a specific process. The control law is based on minimizing the cost function as follows:

$$\begin{aligned} J_k = \sum_{j=1}^{p} &(y(k+j|k) - y^{sp})^\top Q(y(k+j|k) - y^{sp}) \\ &+ \sum_{j=0}^{m-1} (\Delta u(k+j|k))^\top R(\Delta u(k+j|k)) \end{aligned} \tag{4.3}$$

This is used so that from the moment k to the moment $k+m-1$, the sequence of control efforts u is calculated. At the moment $k+p$ the output y_{sp} must be reached. p is the prediction horizon, m is the control horizon, $\Delta u(k+j|k) = u(k+j|k) - u(k+j-1|k)$, $Q > 0$ and $R > 0$ which are matrices with the correct dimensions for the problem. Since

after sample $k+m$, the control effort is null, it is possible to write:

$$\bar{y}(k) = \Phi x(k) + \Gamma \Delta u_k; \Delta u_k = \begin{bmatrix} \Delta u(k|k) \\ \Delta u(k+1|k) \\ \vdots \\ \Delta u(k+m-1|k) \end{bmatrix} \tag{4.4}$$

with:

$$\Phi = \begin{bmatrix} CA \\ CA^2 \\ \vdots \\ CA^p \end{bmatrix} \tag{4.5}$$

and

$$\Gamma = \begin{bmatrix} CB & 0 & \dots & 0 \\ CAB & CB & \dots & 0 \\ \vdots & \vdots & \ddots & \vdots \\ CA^{p-1}B & CA^{p-2}B & \dots & CA^{p-m}B \end{bmatrix}. \tag{4.6}$$

It is possible to write Q and R as $\bar{Q} = diag\left[\underbrace{Q \dots Q}_{p}\right]$ and $\bar{R} = diag\left[\underbrace{R \dots R}_{m}\right]$. Besides that, y^{sp} is the set point for all the predictions and $\bar{y}^{sp} = \left[\underbrace{y^{sp^\top} \dots y^{sp^\top}}_{p}\right]^\top$ is the set point vector. Rewriting the cost function as:

$$\begin{aligned} J_k^{MPC} &= (\Phi x(k) + \Gamma \Delta u_k - \bar{y}^{sp})^\top \bar{Q} (\Phi x(k) \\ &+ \Gamma \Delta u_k - \bar{y}^{sp}) + \Delta u_k^\top \bar{R} \Delta u_k. \end{aligned} \tag{4.7}$$

Then, transforming the objective function to its quadratic form:

$$J_k^{MPC} = \Delta u_k^\top H \Delta u_k + 2 c_f^\top \Delta u_k + c \tag{4.8}$$

where:

$$H = \Gamma^\top \bar{Q}\Gamma + \bar{R}; \tag{4.9}$$

$$c_f^\top = (\Phi x(k) - \bar{y}^{sp})^\top \bar{Q}\Gamma; \tag{4.10}$$

$$c = (\Phi x(k) - \bar{y}^{sp})^\top \bar{Q}(\Phi x(k) - \bar{y}^{sp}). \tag{4.11}$$

Finding Δu_k that minimizes J_k^{MPC}, considering $-\Delta u_{max} \leq \Delta u(k+j|k) \leq \Delta u_{max}$ and $u_{min} \leq u(k+j|k) \leq u_{max}$ with $j = 0, 1, \ldots, m-1$, the control law of MPC is obtained.

4.2 Infinite Horizon Model Predictive Control

In the infinite horizon MPC it is assumed that the set points of the outputs are the origin. That is equivalent to say that the desired steady-state of the system in this project is considered as known and tracking the output can be solved by turning this problem into a regulatory problem, by redefining the state variables.

Similarly to MPC, to accomplish IHMPC control function it is needed to use specific models. The model that is going to be used in this work is the Output Prediction Oriented Model known as OPOM. The details of this model can be found on (MARTINS M. A.; ODLOAK, 2016).

4.2.1 IHMPC Design

Consider the system model as follows, where $C = I$, so the state is assumed to be measured, and x and u are deviation variables based on the steady-state.

$$\begin{aligned} x(k+1) &= Ax(k) + B\Delta u(k) \\ y(k) &= Cx(k) \end{aligned} \tag{4.12}$$

The optimization problem is described in the next equation (ODLOAK, 2004):

$$\begin{aligned} J_k^{IHMPC} = \sum_{j=0}^{\infty} &((y(k+j|k)) - y^{sp} - \delta_y)^\top Q(y(k+j|k) - y^{sp} - \delta_y) \\ &+ \sum_{j=0}^{m-1} (\Delta u(k+j|k))^\top R(\Delta u(k+j|k)) + \delta_u^\top S_y \delta_y \end{aligned} \tag{4.13}$$

δ_y are slack variables and they guarantee that each output variable has its slack variable ensuring feasible solutions once the control law converges to an expression that is based on equality constraints. In other words, the control solution generates values for the control input Δu and slack variables δu, where S_y is the matrix containing all the weights related to them.

Splitting the first term of the previous equation into two, we can rewrite J_k^{IHMPC} as follows.

$$\begin{aligned} J_k^{IHMPC} = & \sum_{j=0}^{m+\theta_{max}} (y(k+j|k) - y^{sp} - \delta_y)^\top Q(y(k+j|k) - y^{sp} - \delta_y) \\ & + \sum_{j=m+\theta_{max}+1}^{\infty} (y(k+j|k) - y^{sp} - \delta_y)^\top Q(y(k+j|k) - y^{sp} - \delta_y) \\ & + \sum_{j=0}^{m-1} (\Delta u(k+j|k))^\top R(u(k+j|k)) + \delta_u^\top S_y \delta_y \end{aligned} \tag{4.14}$$

$m + \theta_{max}$ is the prediction horizon used to calculate the vector of output prediction that can be written as $\bar{y}(k) = \bar{A}x(k) + \bar{B}\Delta u_k$. Δu_k contains the control signals as below, similar to MPC described in the last section.

$$\Delta u_k = \begin{bmatrix} \Delta u(k|k) \\ \Delta u(k+1|k) \\ \vdots \\ \Delta u(k+m-1|k) \end{bmatrix} \tag{4.15}$$

The matrix $\bar{A}$ and $\bar{B}$ are composed as follows:

$$\bar{A} = \begin{bmatrix} C \\ CA \\ \vdots \\ CA^m \\ \vdots \\ CA^{m+\theta_{max}} \end{bmatrix} \tag{4.16}$$

$$\bar{B} = \begin{bmatrix} 0 & 0 & \dots & 0 \\ CB & 0 & \dots & 0 \\ \vdots & \vdots & \ddots & \vdots \\ CA^{m-1}B & CA^{m-2}B & \dots & CB \\ \vdots & \vdots & \ddots & \vdots \\ CA^{m+\theta_{max}-1}B & CA^{m+\theta_{max}-2}B & \dots & CA^{\theta_{max}}B \end{bmatrix} \tag{4.17}$$

In order to rewrite the first term of equation (4.14), it is necessary to create an output set-point vector $\bar{y}^{sp}$ and a supporting vector for the slack variables and adjust the Q matrix to a new $\bar{Q}_y$. Next, we have the structure of each of these elements.

$$\bar{y}^{sp} = \left[\underbrace{y^{sp^\top} \dots y^{sp^\top}}_{m+\theta_{max}+1} \right]^\top \tag{4.18}$$

$$\bar{I}_{ny} = \left[\underbrace{I_{ny} \dots I_{ny}}_{m+\theta_{max}+1} \right]^\top \tag{4.19}$$

$$\bar{Q}_y = diag \left[\underbrace{Q \dots Q}_{m+\theta_{max}+1} \right]^\top \tag{4.20}$$

Using this to recalculate the first term of J_k^{IHMPC}:

$$\begin{aligned} \sum_{j=0}^{m+\theta_{max}} (y(k+j|k) - y^{sp} - \delta_y)^\top Q (y(k+j|k) - y^{sp} - \delta_y) = \\ (\bar{A}x(k) + \bar{B}\Delta u_k - \bar{y}^{sp} - \bar{I}_{ny}\delta_y)^\top \bar{Q}_y (\bar{A}x(k) + \bar{B}\Delta u_k - \bar{y}^{sp} - \bar{I}_{ny}\delta_y) \end{aligned} \tag{4.21}$$

Now using OPOM, j can be written as follows for any moment after $m+\theta_{max}$, considering the definitions of x^s, x^d and Ψ as detailed on (MARTINS M. A.; ODLOAK, 2016) and :

$$y(k+m+\theta_{max}+j|k) = x^s(k+m+\theta_{max}|k) + \Psi x^d(k+m+\theta_{max}+j|k). \tag{4.22}$$

Using (4.22) to rewrite the second therm of J_k^{IHMPC} we will have:

$$\sum_{j=m+\theta_{max}+1}^{\infty}(y(k+j|k)-y^{sp}-\delta_y)^\top Q(y(k+j|k)-y^{sp}-\delta_y)$$
$$=\sum_{j=1}^{\infty}(x^s(k+m+\theta_{max}|k)+\Psi x^d(k+m+\theta_{max}+j|k)-y^{sp}-\delta_y)^\top$$
$$Q_y(x^s(k+m+\theta_{max}|k)+\Psi x^d(k+m+\theta_{max}+j|k)-y^{sp}-\delta_y). \tag{4.23}$$

If $x^s(k+m+\theta_{max}+j|k)-y^{sp}-\delta_y=0$ this term is bounded. Being F stable the term can be redesigned as follows:

$$\sum_{j=1}^{\infty}(\Psi x^d(k+m+\theta_{max}+j|k))^\top Q_y(\Psi x^d(k+m+\theta_{max}+j|k))=$$
$$\sum_{j=1}^{\infty}(\Psi F^j x^d(k+m+\theta_{max}|k))^\top Q_y(\Psi F^j x^d(k+m+\theta_{max}|k))=$$
$$x^d(k+m+\theta_{max}|k)^\top \underbrace{(\sum_{j=1}^{\infty}F^{j\top}\Psi^\top Q_y\Psi F^j)}_{\bar{Q}_d} x^d(k+m+\theta_{max}|k) \tag{4.24}$$

The solution for matrix $\bar{Q}_d$ can be found by working with the following Lyapunov equation:

$$\bar{Q}_d=F^\top\Psi^\top Q_y\Psi F+F^\top\bar{Q}_dF \tag{4.25}$$

After that, consider:

$$\begin{cases} N_d=[O_{nd\times ny} \quad I_{nd} \quad O_{nd\times\theta_{max}}] \\ N_s=[I_{ny} \quad O_{ny\times nd} \quad O_{ny\times\theta_{max}}] \\ W=[A^{m-1}B \quad A^{m-2}B \quad \dots \quad B] \end{cases} \tag{4.26}$$

it is possible to write the predicted states as follows.

$$\begin{cases} x^d(k+m+\theta_{max}|k)=N_dA^{\theta_{max}}(A^mx(k)+W\Delta u_k) \\ x^s(k+m+\theta_{max}|k)=N_sA^{\theta_{max}}(A^mx(k)+W\Delta u_k) \end{cases} \tag{4.27}$$

Getting back to J_k^{IHMPC}, considering all this development, it can be written as:

$$J_k^{IHMPC} = (\bar{A}x(k) + \bar{B}\Delta u_k - \bar{y}^{sp} - \bar{I}_{ny}\delta_y)^\top \bar{Q}(\bar{A}x(k) + \bar{B}\Delta u_k - \bar{y}^{sp} - \bar{I}_{ny}\delta_y)$$
$$+(N_d A^{\theta_{max}}(A^m x(k) + W\Delta u_k))^\top \bar{Q}_d(N_d A^{\theta_{max}}(A^m x(k) + W\Delta u_k))$$
$$+\Delta {u_k}^\top \bar{R}\Delta u_k + \delta_u^\top S_y \delta_y \quad (4.28)$$

and turned into a quadratic formulation

$$J_k^{IHMPC} = \begin{bmatrix}\Delta u_k & \delta_y\end{bmatrix} \begin{bmatrix}H_{11} & H_{12}\\ H_{21} & H_{22}\end{bmatrix} \begin{bmatrix}\Delta u_k\\ \delta_y\end{bmatrix} + 2\begin{bmatrix}c_{f1} & c_{f2}\end{bmatrix} \begin{bmatrix}\Delta u_k\\ \delta_y\end{bmatrix} + c \quad (4.29)$$

where

$$\begin{cases} H_{11} = \bar{B}^\top \bar{Q}_y \bar{B} + (N_d A^{\theta_{max}} W)^\top \bar{Q}_d (N_d A^{\theta_{max}} W) + \bar{R} \\ H_{12} = -\bar{B}^\top \bar{Q}_y \bar{I}_{ny} \\ H_{21} = H_{12}^\top \\ H_{22} = \bar{I}_{ny}^\top \bar{Q}_y \bar{I}_{ny} + S_y \\ c_{f1} = (\bar{A}x(k) - \bar{y}^{sp})^\top \bar{Q}_y \bar{B} + (N_d A^{\theta_{max}+m} x(k))^\top \bar{Q}_d (N_d A^{\theta_{max}} W) \\ c_{f2} = -(\bar{A}x(k) - \bar{y}^{sp})^\top \bar{Q}_y \bar{I}_{ny} \\ c = (\bar{A}x(k) - \bar{y}^{sp})^\top \bar{Q}_y (\bar{A}x(k) - \bar{y}^{sp}) + (N_d A^{\theta_{max}+m} x(k))^\top \bar{Q}_d (N_d A^{\theta_{max}+m} x(k)). \end{cases} \quad (4.30)$$

To reach the control law, it is necessary to solve the quadratic programming

$$\min_{\Delta u_k, \delta_y} \begin{bmatrix}\Delta u_k & \delta_y\end{bmatrix} \begin{bmatrix}H_{11} & H_{12}\\ H_{21} & H_{22}\end{bmatrix} \begin{bmatrix}\Delta u_k\\ \delta_y\end{bmatrix} + 2\begin{bmatrix}c_{f1} & c_{f2}\end{bmatrix} \begin{bmatrix}\Delta u_k\\ \delta_y\end{bmatrix} \quad (4.31)$$

submitted to:

$$-\Delta u_{max} \leq \Delta u(k+j|k) \leq \Delta u_{max}, j = 0, 1, \ldots, m-1,$$
$$u_{min} \leq u(k+j|k) \leq u_{max}, j = 0, 1, \ldots, m-1,$$
$$N_d A^{\theta_{max}}(A^m x(k) + W\Delta u_k) - y^{sp} - \delta_y = 0. \quad (4.32)$$

4.3 Extremum Seeking Control

Considering the scenario of high complexity systems, the Extremum Seeking Control (ESC) technique is one of the possible solutions (ARIYUR et al., 2003). Extremum

Seeking is a real-time analogical optimizer (KRSTIć; WANG, 2000) in which the algorithm uses only the output for the input's calculation, aiming to guarantee that the output converges to an optimum point.

The technique that is going to be used for ESC is the most common one: by sinusoidal disturbance (KRSTIć; WANG, 2000; ZHANG; ORDÓÑEZ, 2012). So the next step is to prove this algorithm. Considering the block diagram bellow (Figure5) there is a $\theta^\star$ related to the optimum point $f^\star = f(\theta^\star)$ and the estimation error is defined as $\tilde{\theta} = \theta^\star - \hat{\theta}$.

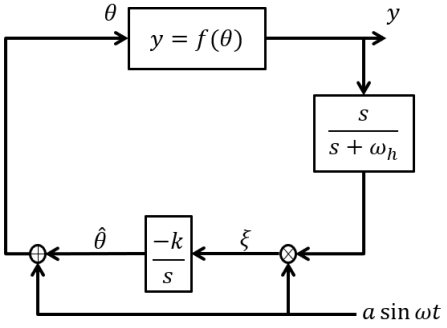

Figure 5: ESC block diagram.

Around the equilibrium point, $f(\theta)$ can be written as:

$$f(\theta) = f^\star + \frac{f''}{2}(\theta - \theta^\star)^2. \tag{4.33}$$

And from the block diagram $\theta = \hat{\theta} + a\sin(\omega t)$. So the estimation error is equivalent to

$$\theta - \theta^\star = a\sin(\omega t) - \tilde{\theta}, \tag{4.34}$$

and, substituting in (4.33), results in

$$f(\theta) = f^\star + \frac{f''}{2}(\hat{\theta} - a\sin(\omega t))^2. \tag{4.35}$$

Expanding it is possible to reach the equation below.

$$y = f^\star + \frac{a^2 f''}{4}(1 + \cos(2\omega t)) + \frac{f''}{2}\tilde{\theta}\sin(\omega t). \tag{4.36}$$

By design, it is possible to remove the constant terms from the previous equation as the high-pass filter cuts off the frequencies below the chosen ESC frequency.

$$y_{hp} = \frac{f''}{2}\tilde{\theta}^2 - af''\tilde{\theta}\sin(\omega t) + \frac{a^2 f''}{4}\cos(2\omega t). \tag{4.37}$$

And as a last step, y_{hp} is multiplied by $a\sin(\omega t)$ and goes through the integrator. As it

is shown in (ARIYUR et al., 2003), the average of the output integrator is

$$\dot{\tilde{\theta}} \approx \frac{-a^2 k f''}{2}\tilde{\theta}, \tag{4.38}$$

if $kf'' > 0$, it is stable, so $\tilde{\theta} \to 0$, that implies $\hat{\theta} \to \theta^\star$, which proves the convergence of the method.

Once the method is valid, we are going through the controller schema design. Firstly it is necessary to guarantee that ESC's frequency is higher than the natural frequencies of the plant. This hypothesis is viable once the idea is to keep a high frequency, so it becomes possible to see in the output of the plant the effects of this oscillation. In this case, we are using ESC as a direct controller and the main goal is to minimize the quadratic error. The error is equal to zero in most systems.

The block diagram in Figure 6 shows this schema.

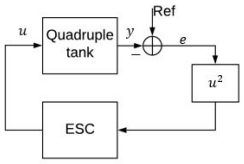

Figure 6: Direct ESC control block diagram.

The controller is considered decoupled, and every ESC implementation for each output uses the same parameters. This can be checked in Figure 7, where $\phi = 0$ to $i = 1$ and $\phi = \pi/2$ to $i = 2$.

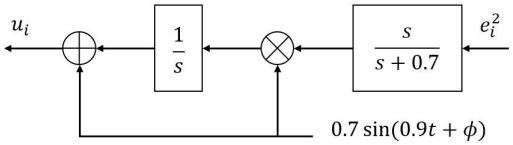

Figure 7: Direct ESC algorithm by channel.

The control effort constraint for ESC is $0\text{V} \leq u \leq 10\text{V}$. It actuates directly in the plant.

5 RESULTS

Aiming to test the theory studied, a set of Matlab codes was written. Firstly it was done some tests to reach the PRBS and the best solution is already explained in Chapter 3. With this PRBS as input, it was possible to test all identification models shown in Chapter 3, following sections considering the data that was collected by tests in the practical plant. The result with the best FIT in that test was chosen as the one to test MPC and IHMPC. The results are compared to the ones that ESC provides.

5.1 Identification

As cited in Section 3, the inputs for both pumps were PRBS signals. These input signals were presented in Figure 3 and in Figure 4. Two-thirds of the outputs were designated for identification. The other third was used as validation data.

The *ident* tool from MatLab was used to create the models. Table 1 and Table 2 show the FIT values for lower order considering y_1 and y_2 respectively.

Table 1: FIT values for y_1.

Order	FIT ARX	FIT ARMAX	FIT OE	FIT BJ
1	34.86%	37.61%	15.99%	82.91%
2	25.68%	26.74%	60.55%	-60.55%
3	24.85%	56.56%	25.46%	88.98%
4	24.53%	34.57%	25.15%	93.72%

Table 2: FIT values for y_2.

Order	FIT ARX	FIT ARMAX	FIT OE	FIT BJ
1	36.58%	38.59%	28.58%	88.76%
2	28.13%	30.96%	53.97%	71.95%
3	28.26%	48.44%	-207.40%	87.33%
4	28.79%	36.94%	-54.52%	91.85%

In Figure 8 is shown the measured and the simulated models outputs for tank 1 (y_1)

and for tank 2 (y_2) considering the order 4. In order to determine which one of the models represents the process the best, it was used the FIT coefficient as explained. The legend describes the model and its FIT. For all models the orders were fixed at 4, considered the best FIT on the previous tables, so it would be more reasonable to choose the most effective one between them.

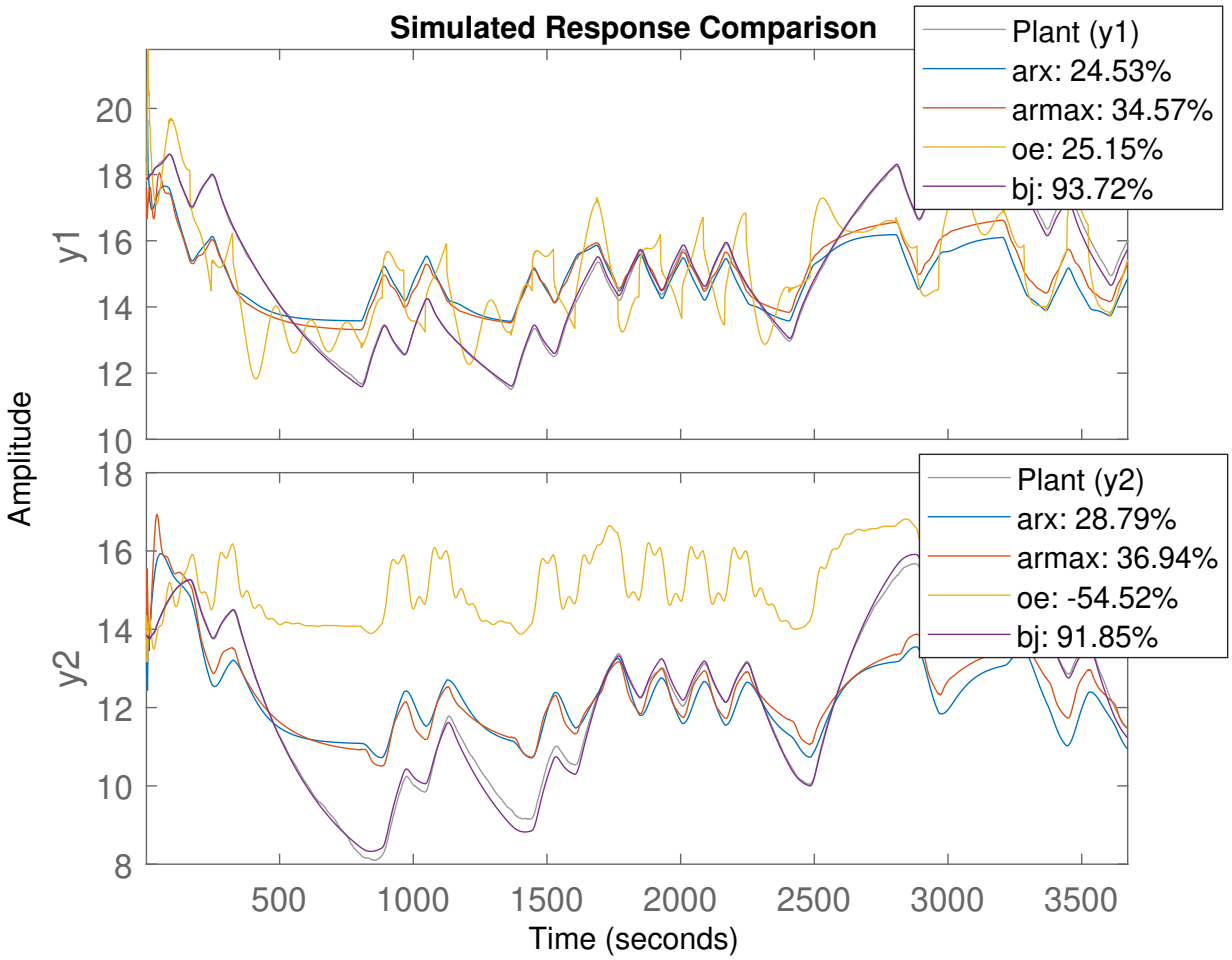

Figure 8: Measured and simulated values for output y1 and y2.

Considering the generated models, the best-obtained result was the BJ model with 4th order. So we are using this model to test the control techniques from now on. Figure 9shows the step response for this model.

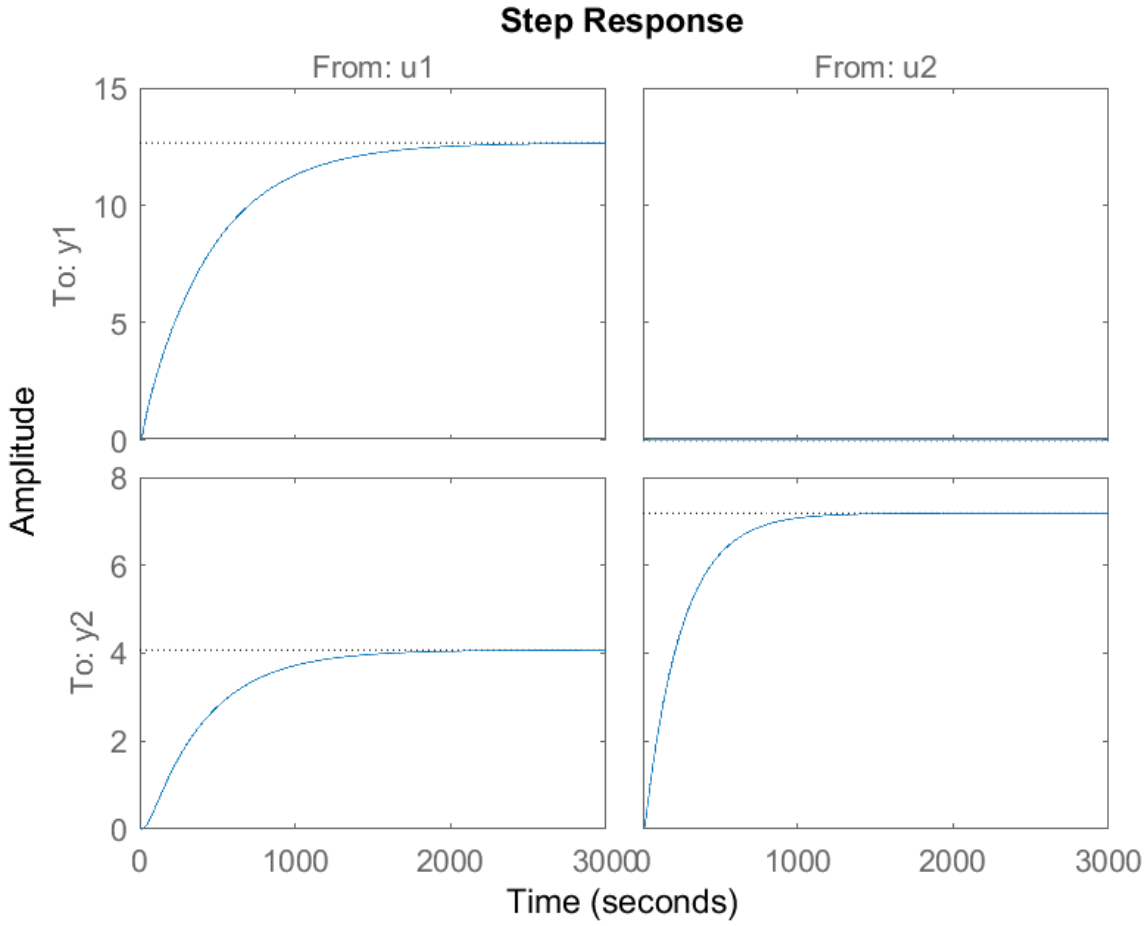

Figure 9: Step response for the BJ model.

5.2 MPC

In order to test the MPC, three experiments were designed and both the phenomenological and the identified models were applied. The main parameters for the MPC are the following ones:

$$\begin{aligned} n_u &= 2 \\ n_y &= 2 \\ T &= 2 \\ p &= 70 \\ m &= 40 \\ q &= 10 * [15, 15] \\ r &= 0.5 * [1, 1] \end{aligned} \tag{5.1}$$

5.2.1 Case a

The first experiment tests the reference tracking using a step response. The quadruple tank is working at the operation point and steps of 2 cm are added to or subtracted from the reference on different instants as shown in Figure 10 for the phenomenological model and in Figure 12 for the identified model. Figures 11 and 13 show the control effort for each case.

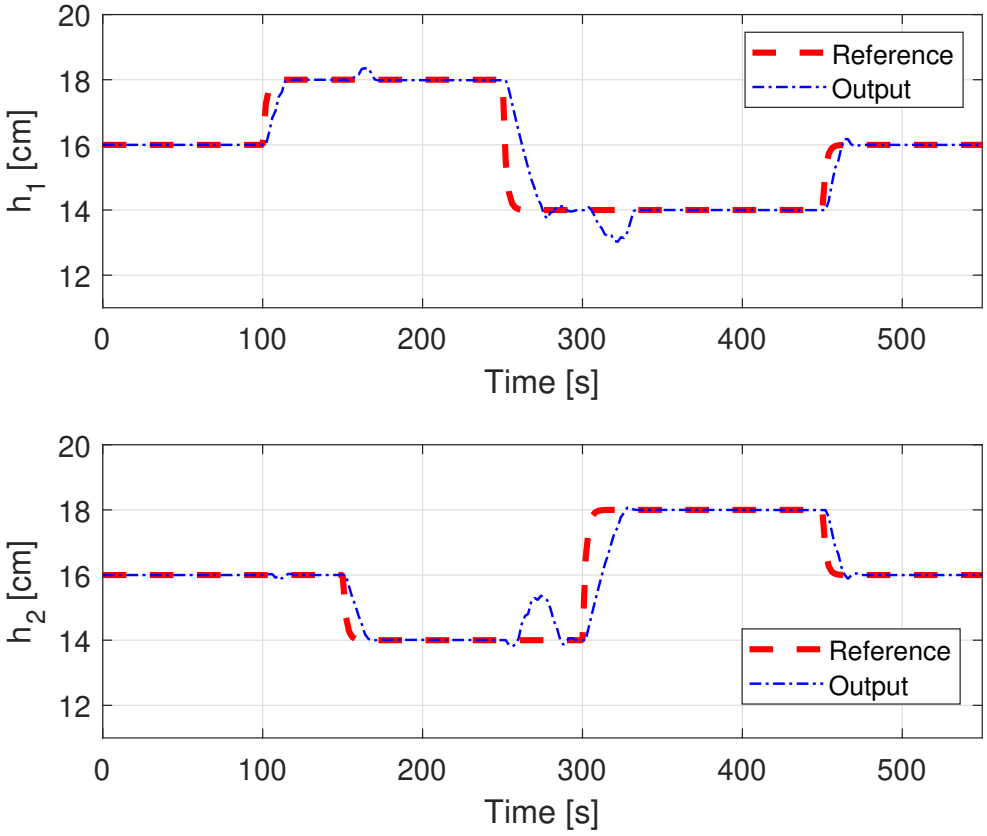

Figure 10: Step reference tracking for tanks 1 and 2 to the phenomenological model.

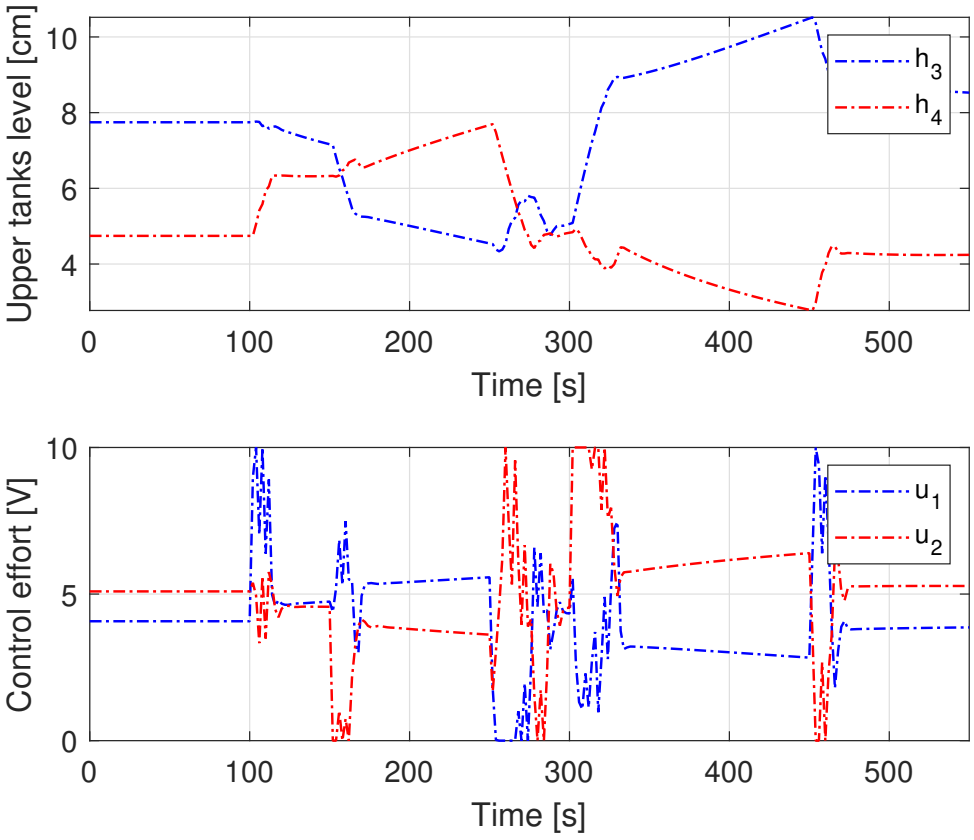

Figure 11: Step reference tracking control effort for tanks 1 and 2 to the phenomenological model.

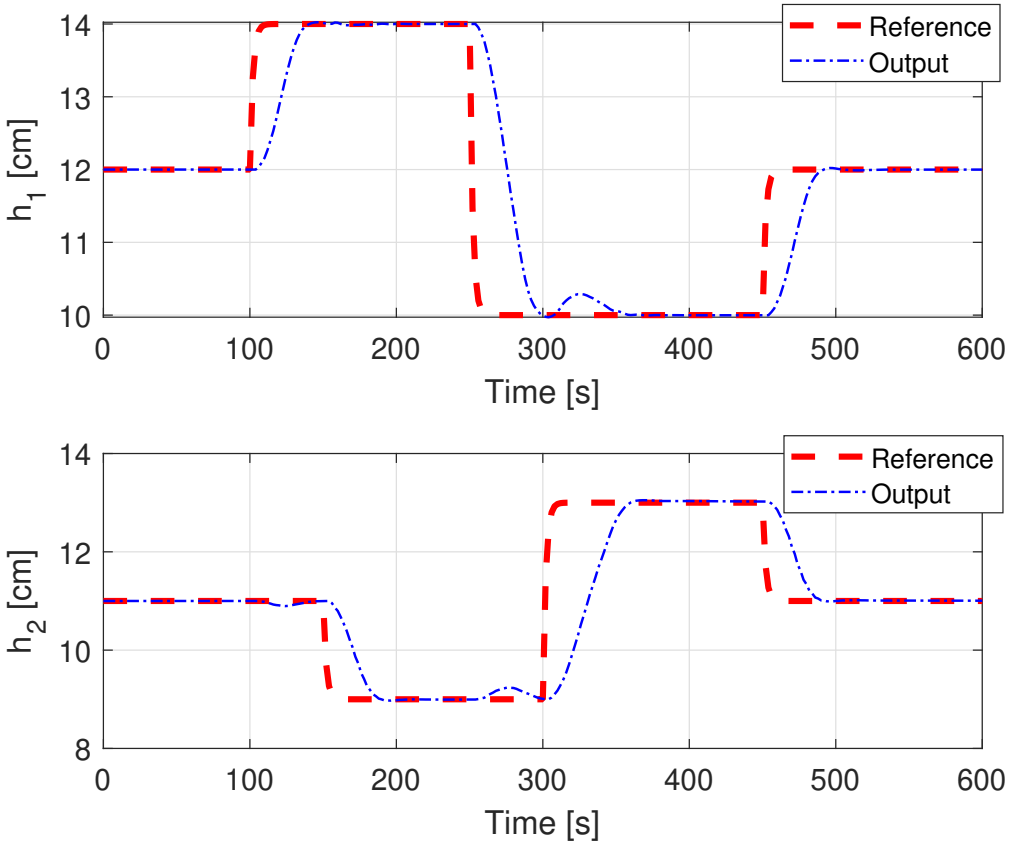

Figure 12: Step reference tracking for tanks 1 and 2 to the identified model.

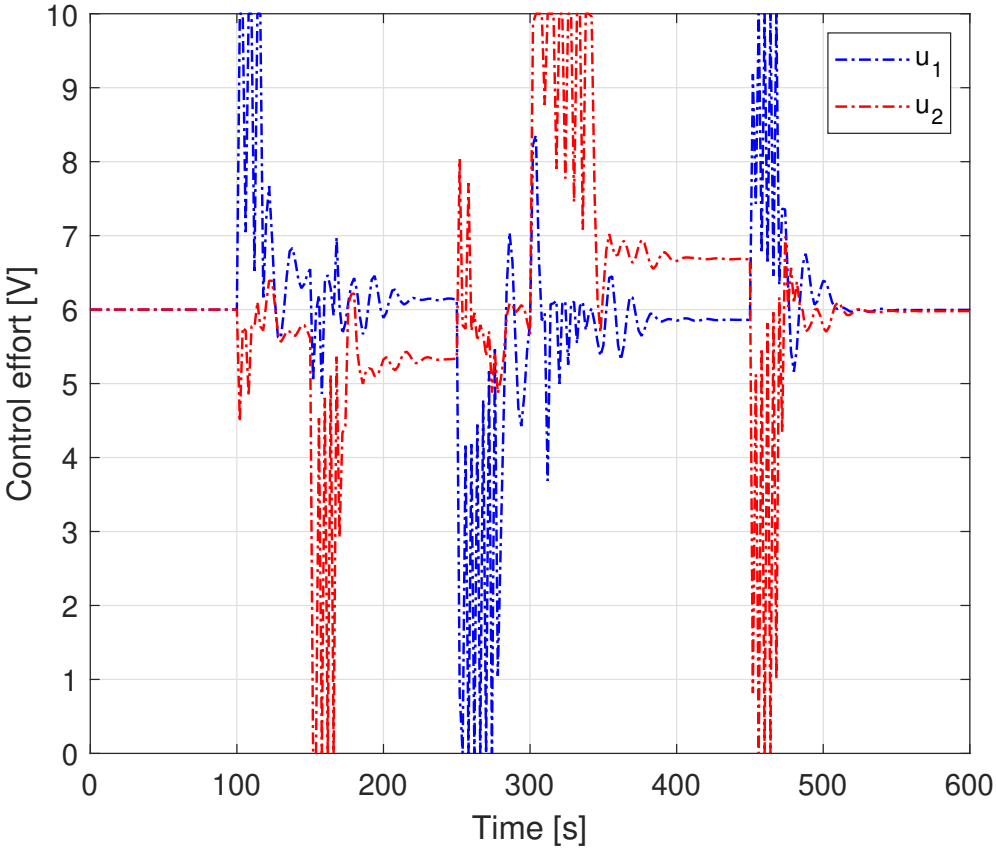

Figure 13: Step reference tracking control effort for tanks 1 and 2 to the identified model.

5.2.2 Case b

The second experiment tests the reference tracking but using a sinusoidal signal, so we have a comparison with a different input signal. Similarly, the quadruple tank is working at operation point and the reference changes to a sinusoidal signal with 2cm of amplitude and 10^{-2}Hz of frequency. Figure 14 presents the results for the phenomenological model and Figure 16 for the identified model. Figures 15 and 17 show the control effort for each case.

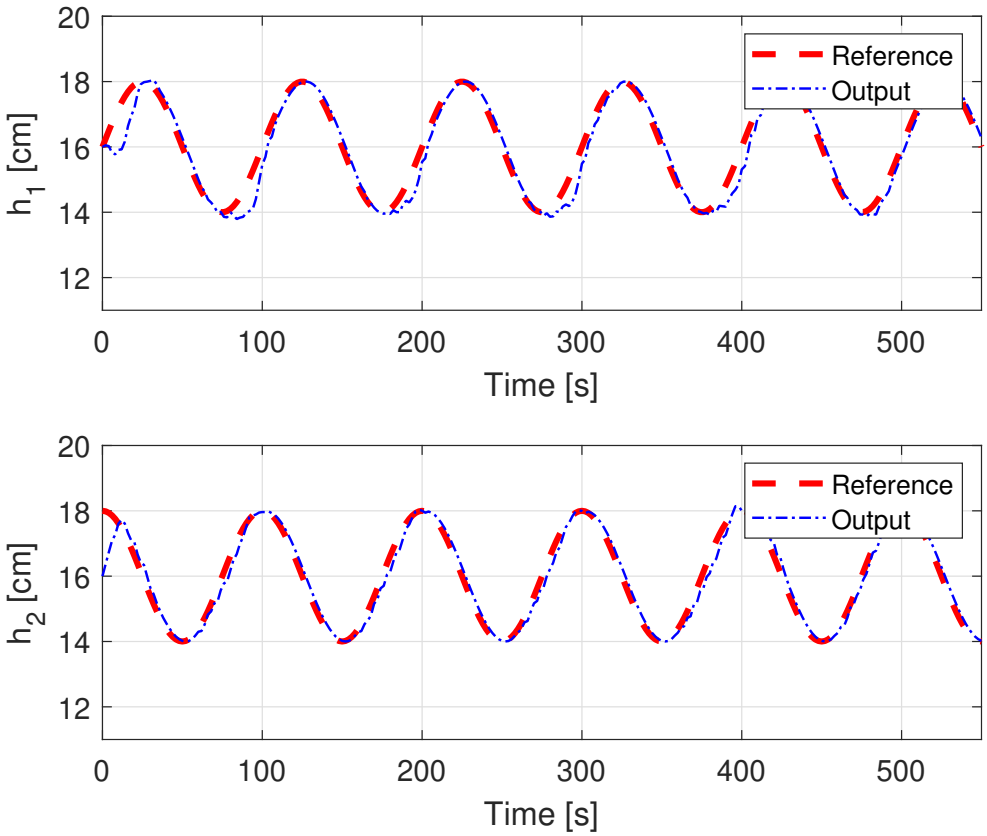

Figure 14: Sinusoidal reference tracking for tanks 1 and 2 to the phenomenological model.

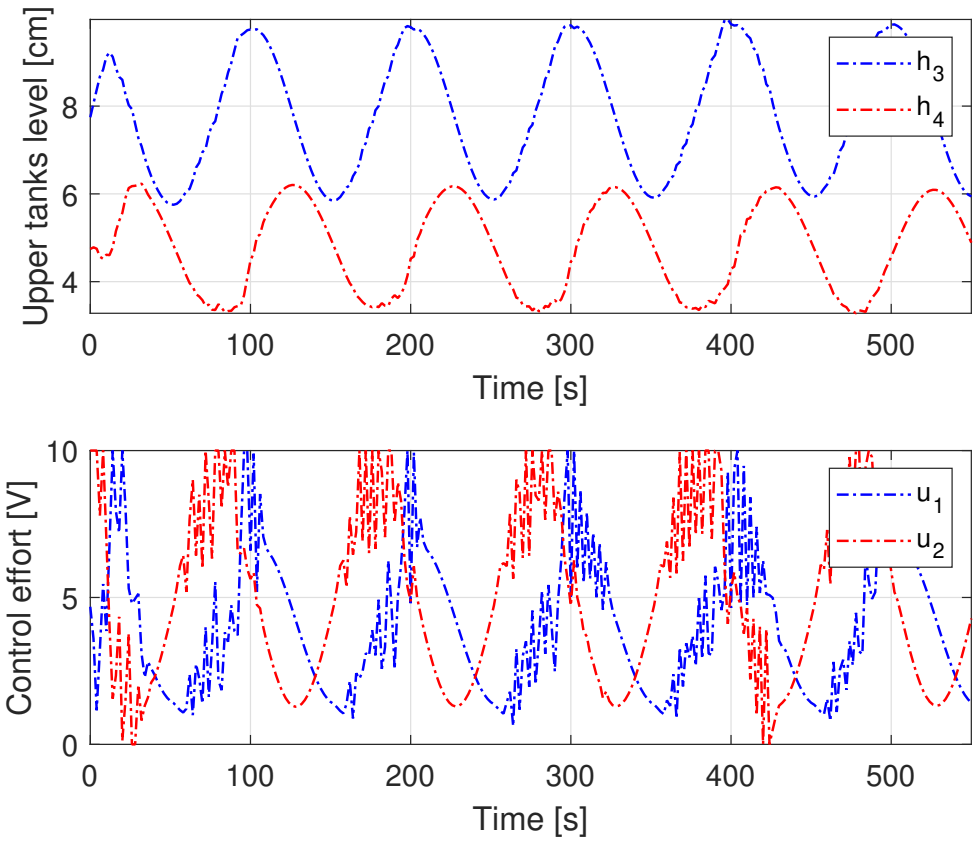

Figure 15: Sinusoidal reference tracking control effort for tanks 1 and 2 to the phenomenological model.

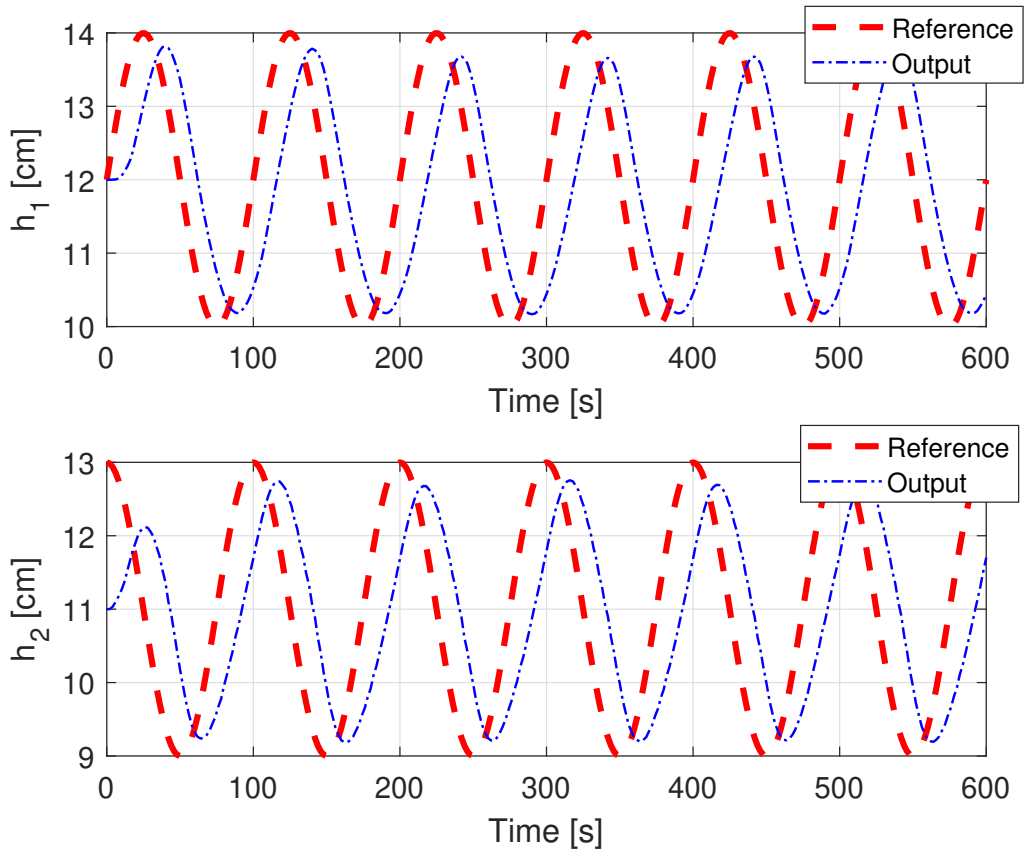

Figure 16: Sinusoidal reference tracking for tanks 1 and 2 to the identified model.

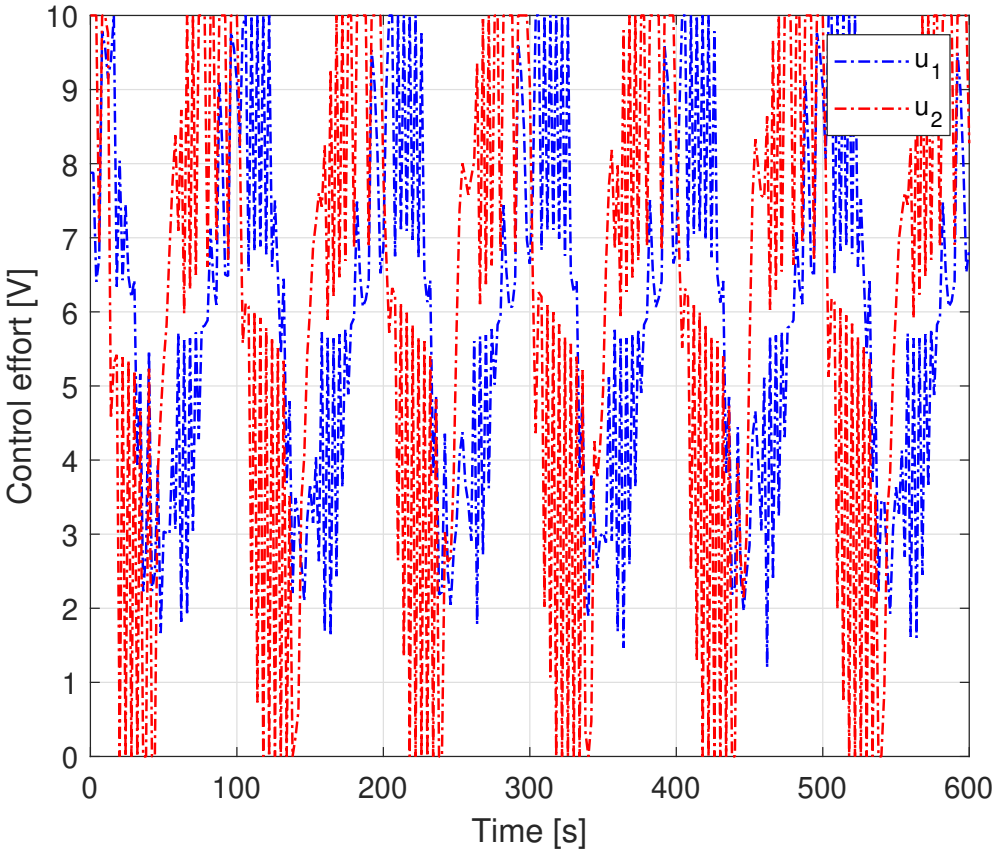

Figure 17: Sinusoidal reference tracking control effort for tanks 1 and 2 to the identified model.

5.2.3 Case c

The third experiment tests the disturbance rejection by watching the effects of an additive disturbance at the output. It is used for that a step signal for the two outputs h_1 and h_2. In Figure 18 is shown the outputs for the phenomenological model and in Figure 19 the equivalent control effort. Figures 20 and 21 show the same views but for the identified model. Figure 22 shows the disturbance.

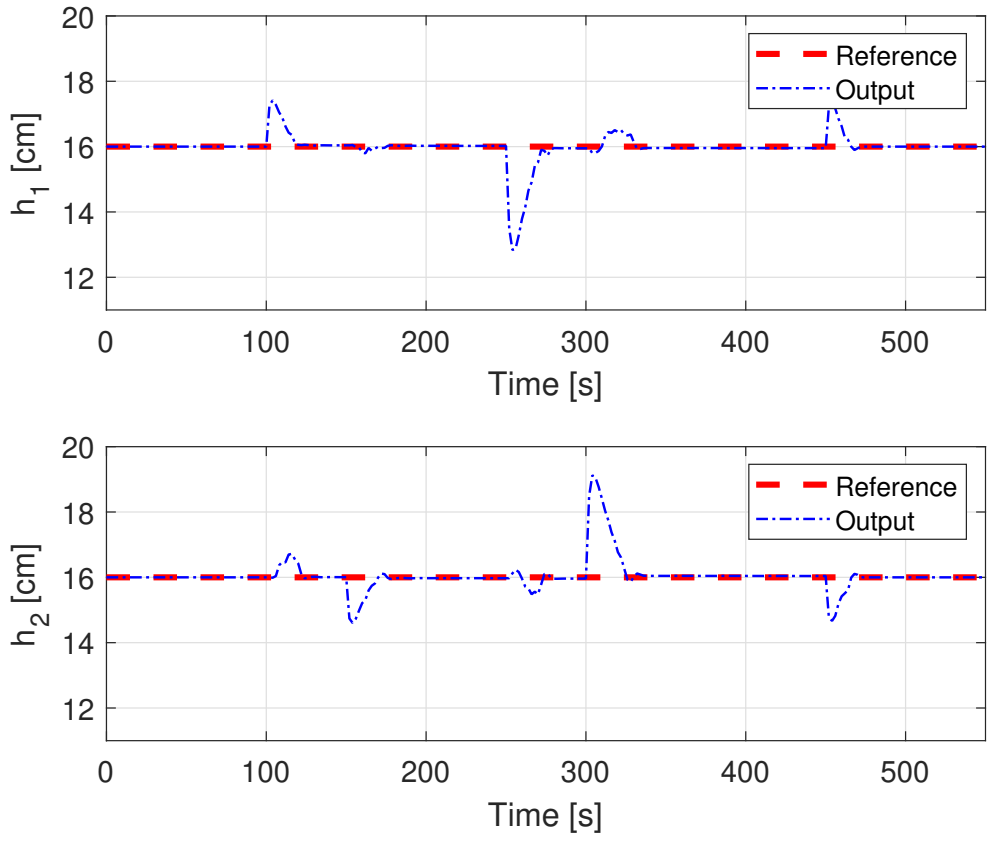

Figure 18: Fixed reference tracking for tanks 1 and 2 to the phenomenological model considering an additive disturbance at the output.

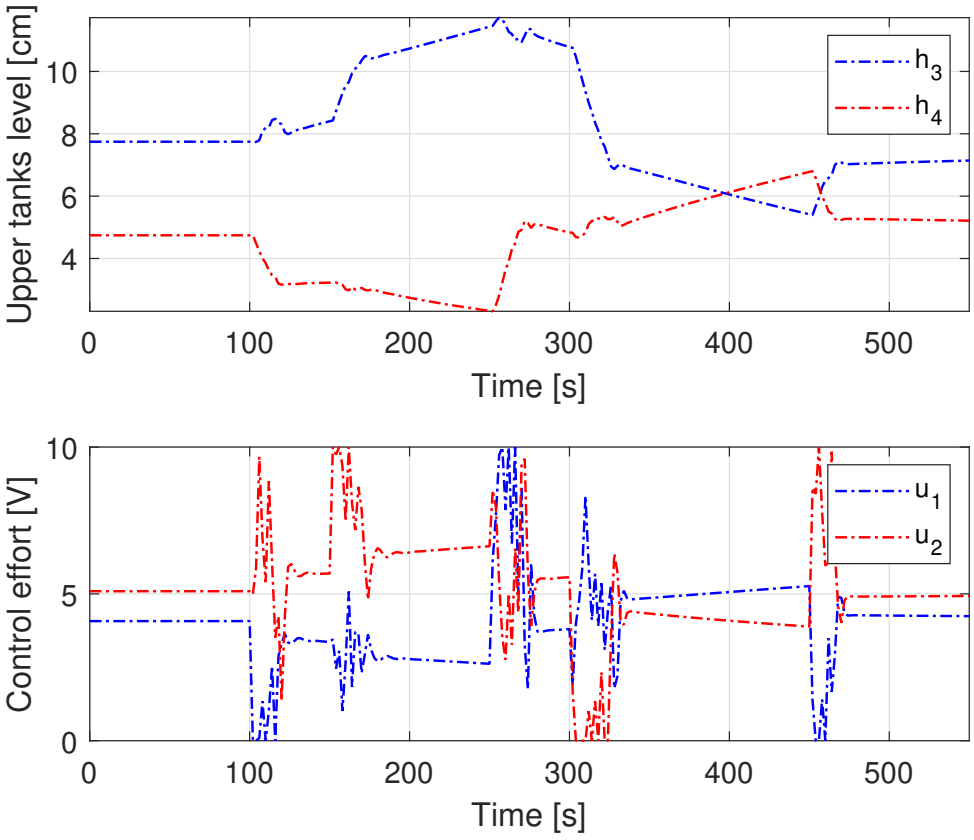

Figure 19: Reference tracking control effort for tanks 1 and 2 to the phenomenological model considering an additive disturbance at the output.

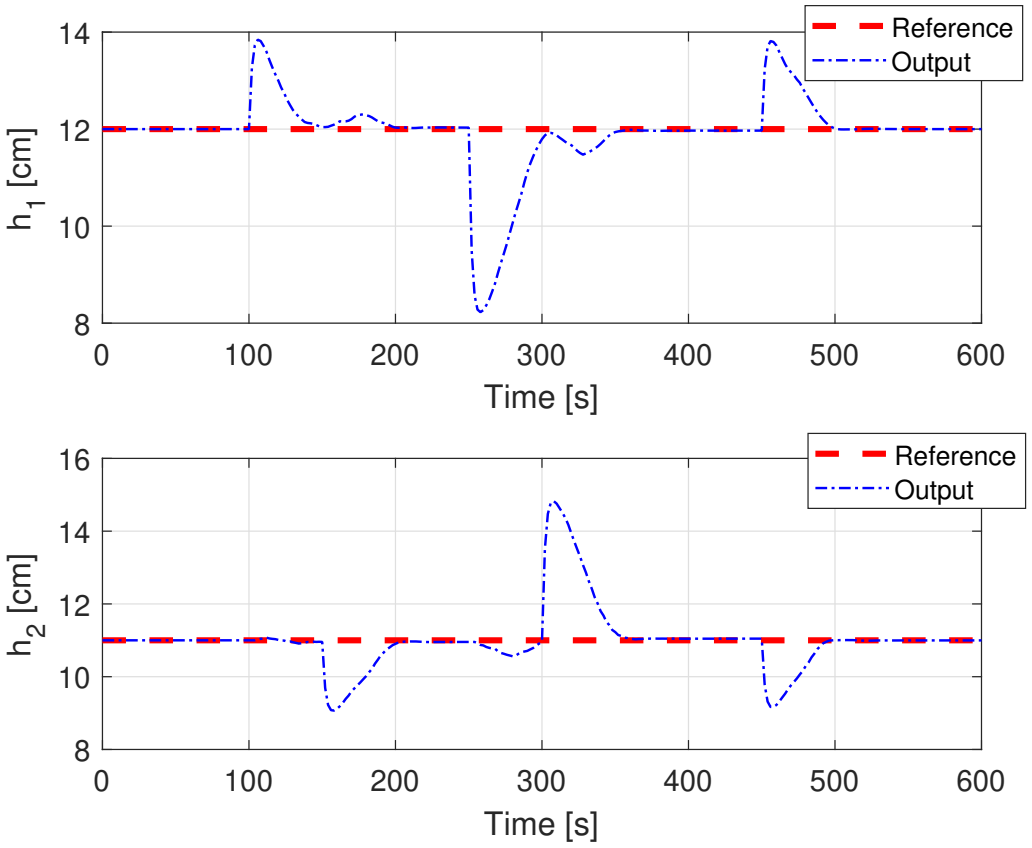

Figure 20: Fixed reference tracking for tanks 1 and 2 to the identified model considering an additive disturbance at the output.

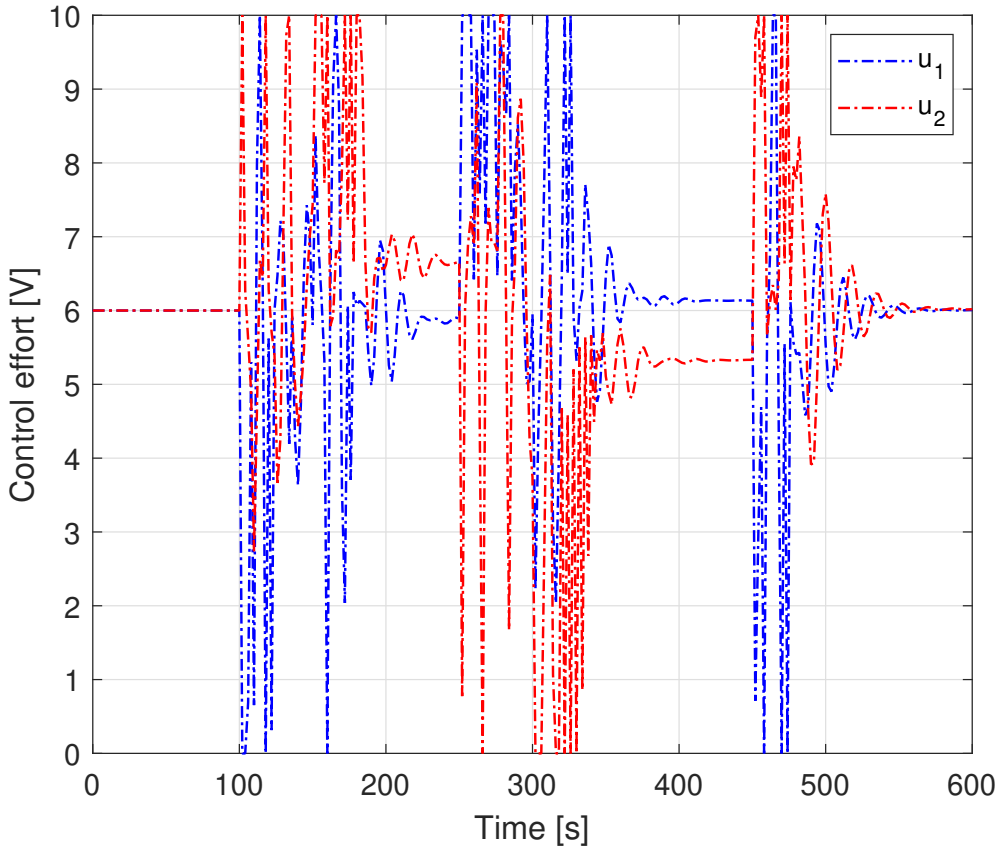

Figure 21: Reference tracking control effort for tanks 1 and 2 to the identified model considering an additive disturbance at the output.

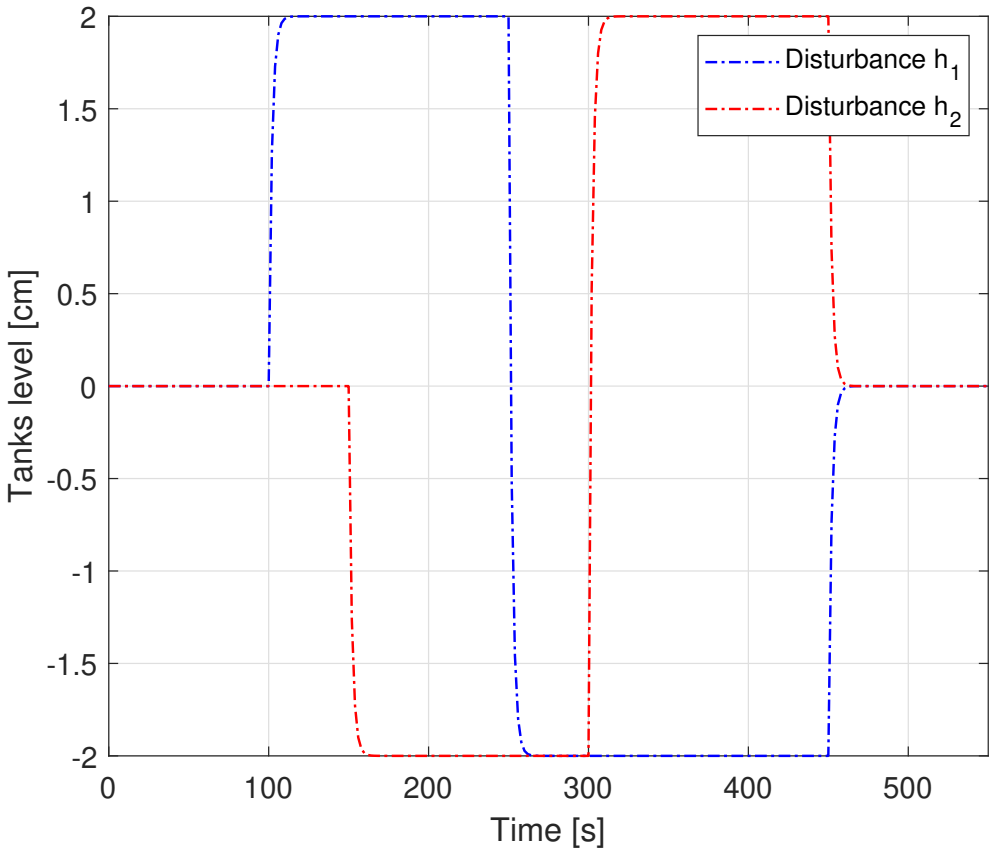

Figure 22: The additive disturbance at the output.

5.3 IHMPC

The implementation of IHMPC was quite similar to the one of MPC. The difference was using the OPOM model to consider the plant dynamics. The best tuning results can be seen in Figure 23 for the outputs and in Figure 24 for the control effort.

The results show that it was not the best control technique for this plant. Firstly, it was really hard to tune the controller. And secondly, even though it was possible to have one of the outputs with a reasonable outcome, the other output did not show the same kind of response. And finally, the controller itself is so slow that would make an industrial plant implementation quite inefficient.

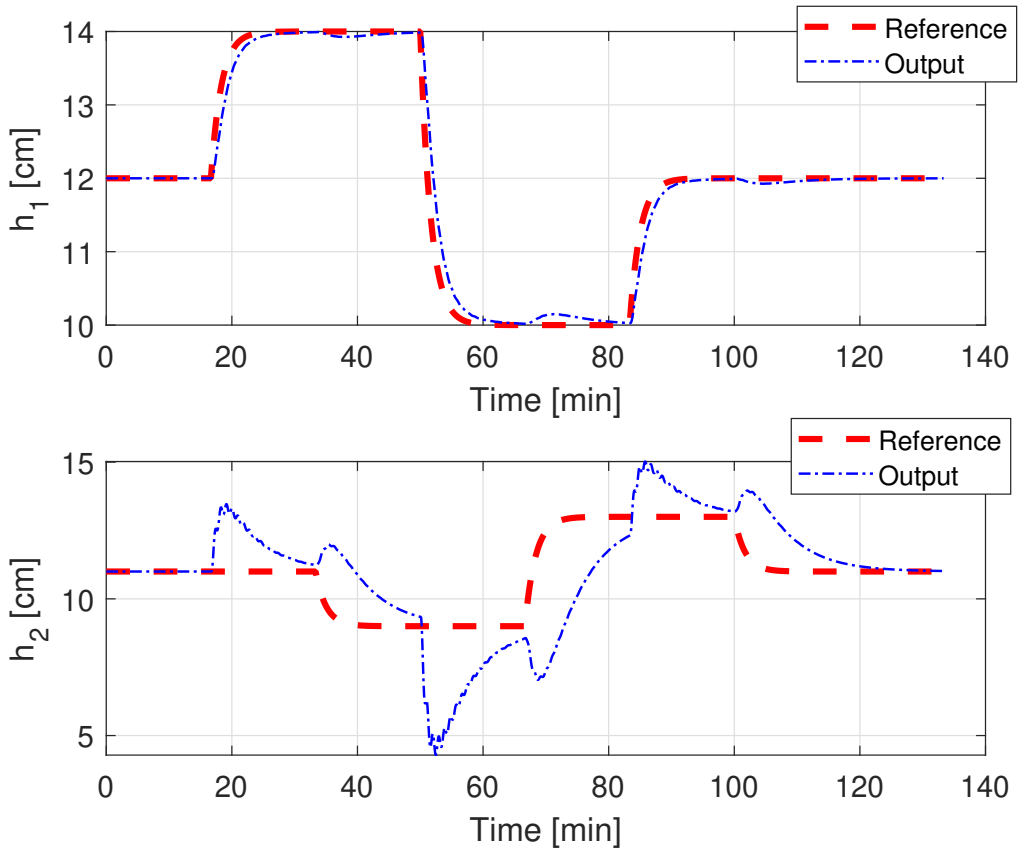

Figure 23: Reference tracking control effort for tanks 1 and 2 to the identified model.

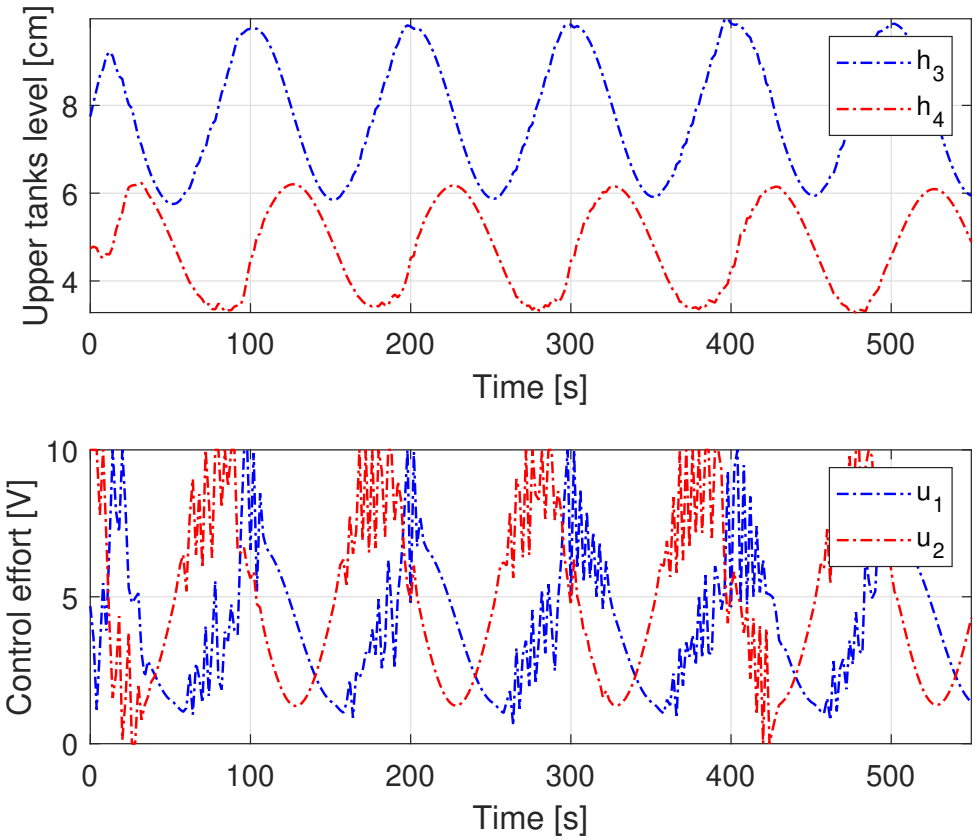

Figure 24: Reference tracking control effort for tanks 1 and 2 using IHMPC.

The main parameters for the IHMPC are the following ones:

$$
\begin{aligned}
n_u &= 2 \\
n_y &= 2 \\
T &= 2 \\
m &= 30 \\
q &= 10 * [15, 15] \\
r &= 0.5 * [1, 1] \\
q &= 10^{-3} * [30, 1] \\
r &= [32, 4] \\
s &= 10^3 * diag([100, 0.01])
\end{aligned}
\tag{5.2}
$$

5.4 ESC

This section presents the simulation results obtained for four distinct cases designed for the plant.

5.4.1 Case a

For the first test, the quadruple tank operates at minimum phase ($\gamma_1 = 0.6$ and $\gamma_2 = 0.6$) and it is used a pulse reference with the initial condition of $h_1 = 9$ cm and $h_2 = 9$ cm. Figure 25 shows the tank levels to the system using ESC as controller. The control effort and the quadratic error are shown in Figure 26. The system presented a good result, so that the tanks 1 and 2 converged to the reference. But, the control effort of this approach is very oscillatory. Note that the control effort presents the sinusoidal variation from the ESC algorithm.

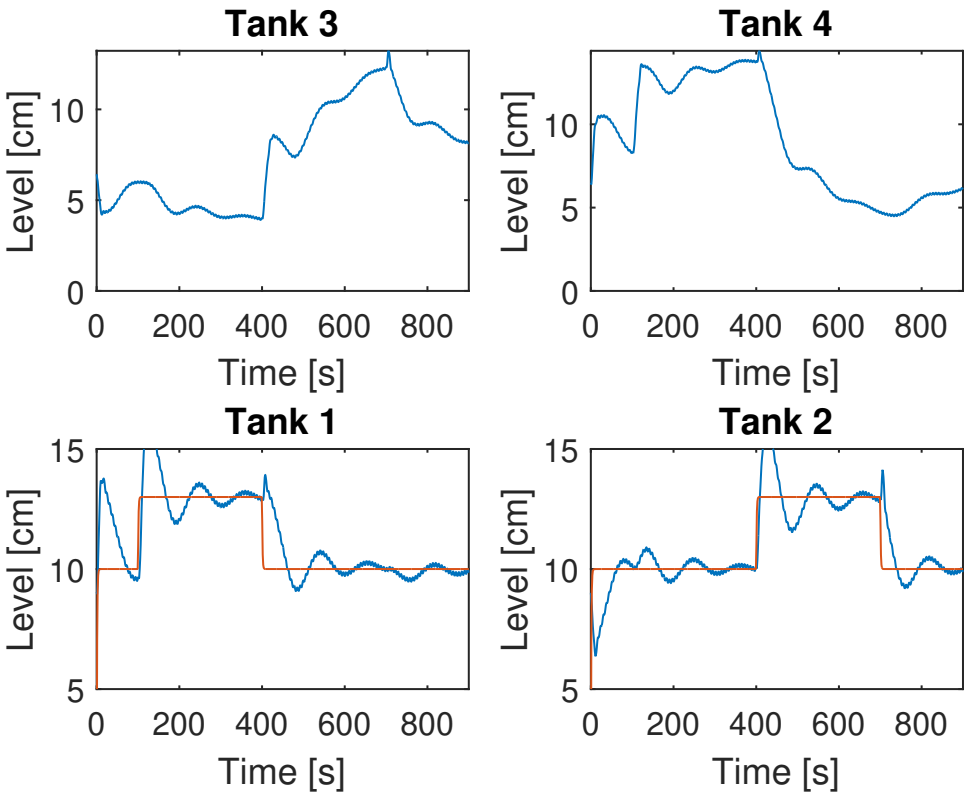

Figure 25: Outputs considering a pulse reference.

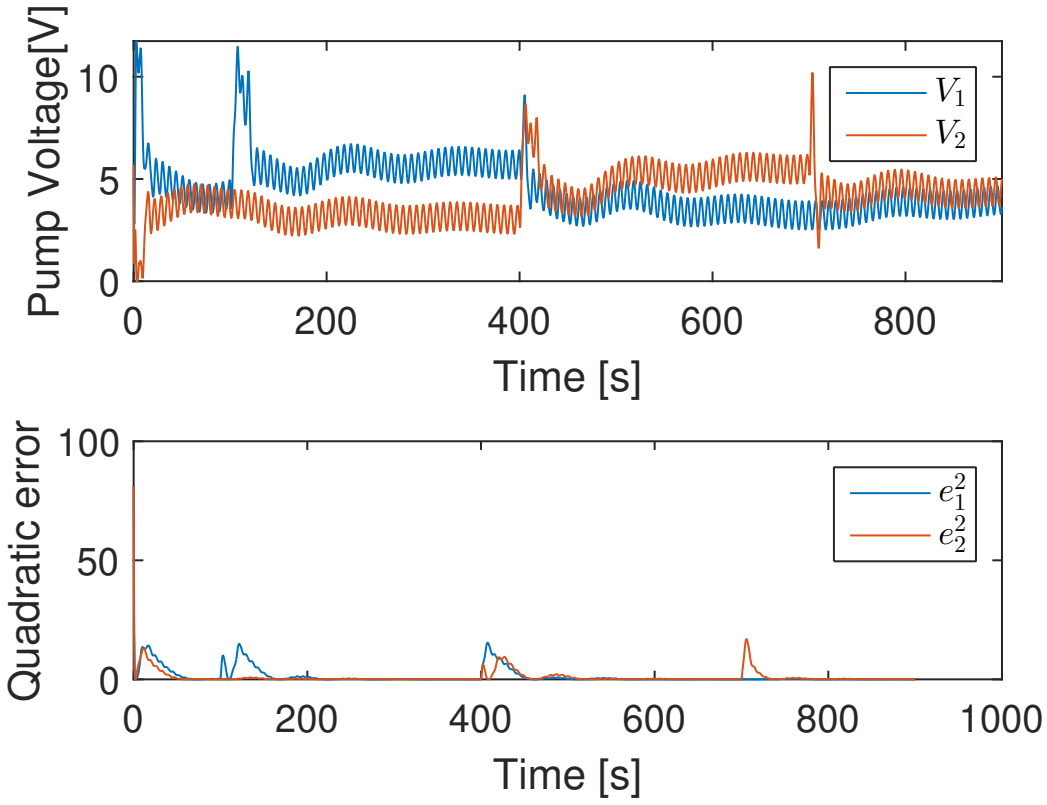

Figure 26: Control effort and quadratic error considering a pulse reference.

5.4.2 Case b

The second experiment considers the same opening of the valve than the case before, but now it is used a sinusoidal reference for each tank with an initial condition for each one being $h = 12$ cm.

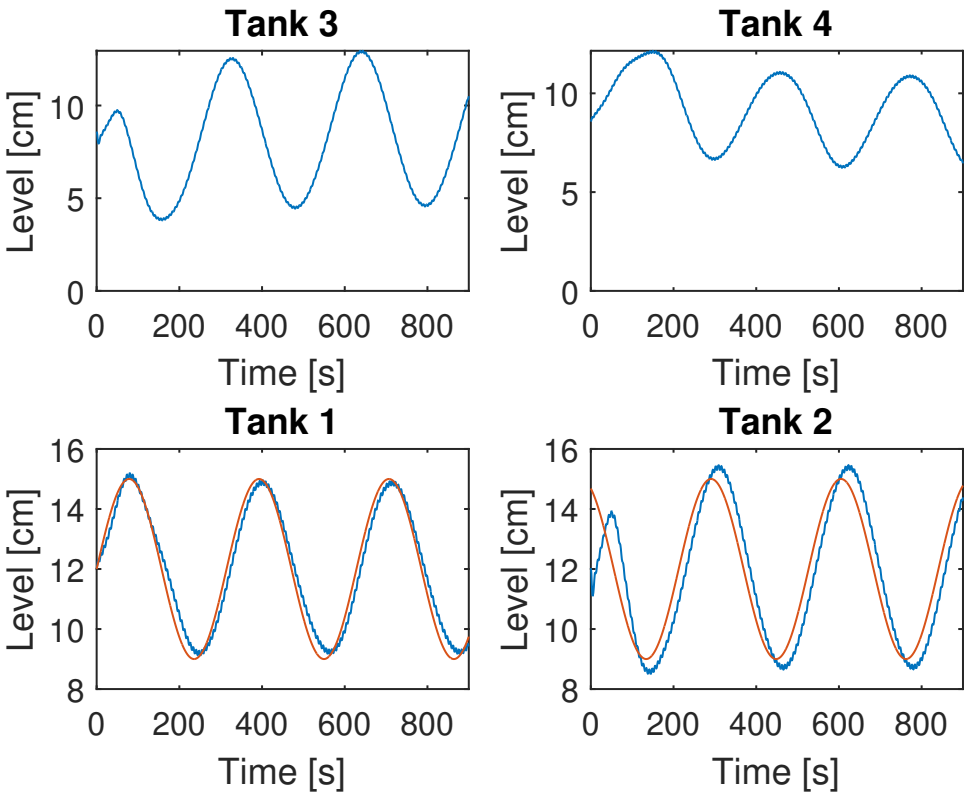

Figure 27: Outputs considering a sinusoidal reference.

The results are shown in Figures 27 and 28 from the non-model based control. Thus the tank 2 had a slightly larger error and with a greater deviation in the initial condition when compared to tank 1, the results were satisfactory.

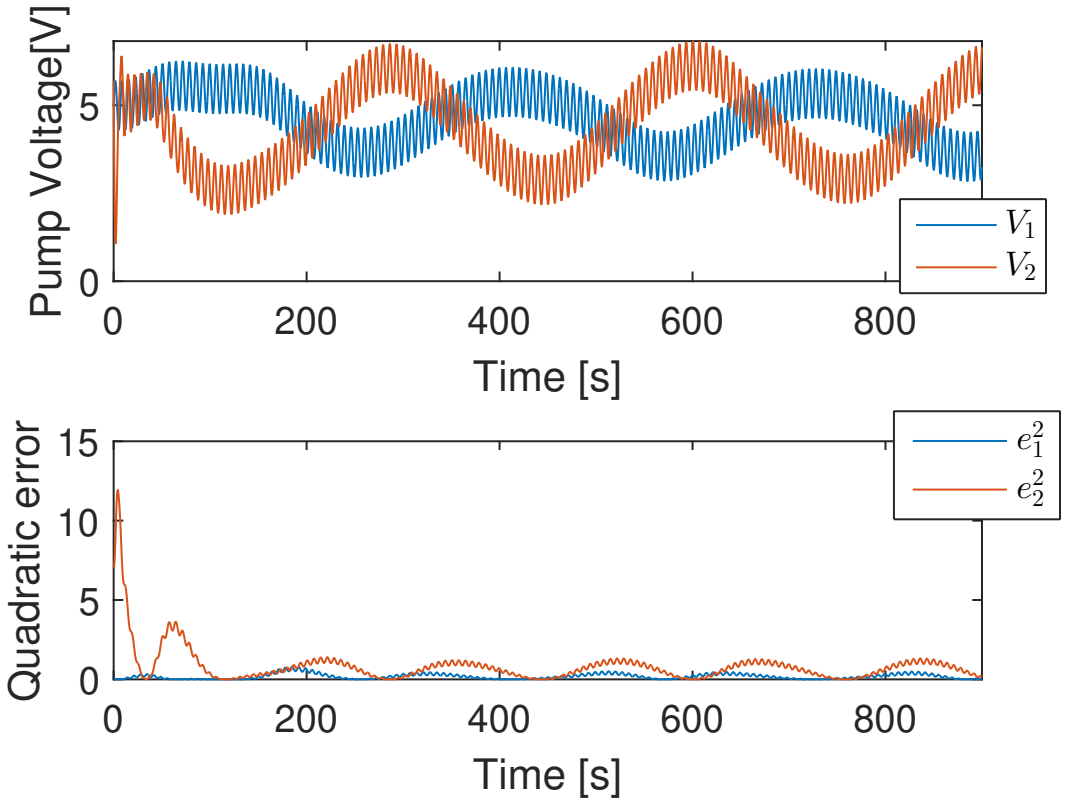

Figure 28: Control effort and quadratic error considering a sinusoidal reference.

5.4.3 Case c

The third case represents the same situation of the case ”a” such as the reference and the initial condition, but now we are considering that γ_1 and γ_2 are time variants. Figure 29 shows these conditions. Note that, in this situation, the system spends a short period in non-minimum phase.

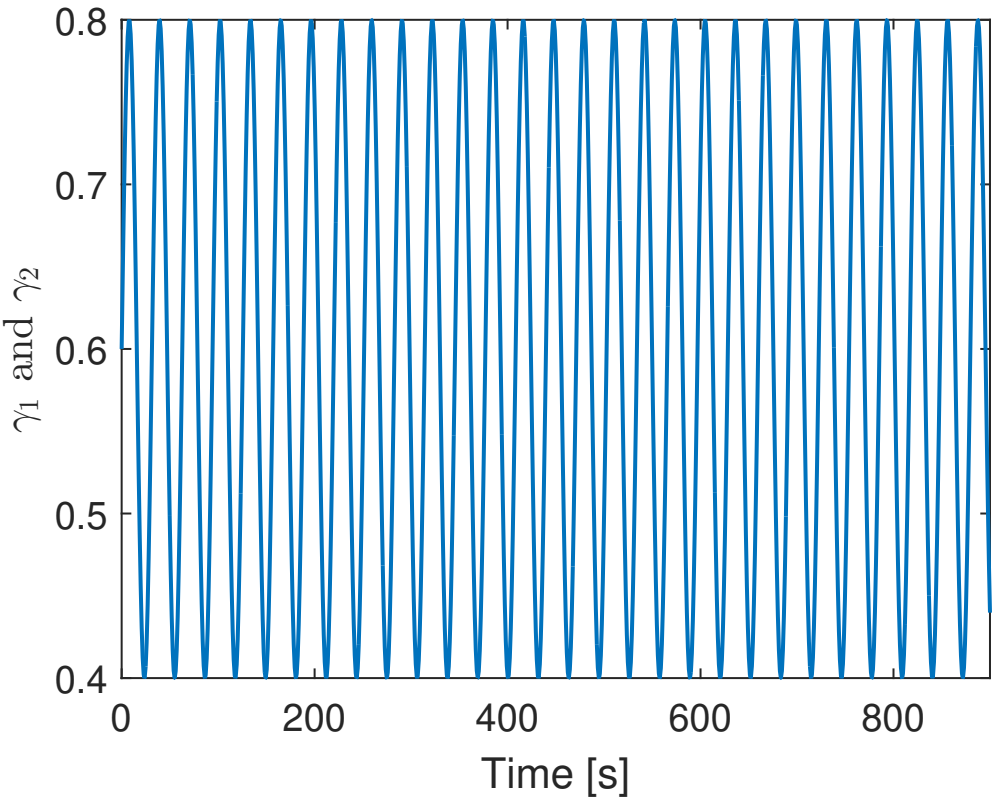

Figure 29: Time variant γ_1 and γ_2 considered in cases ”c” and ”d”.

Figure 30 shows the output system and Figure 31 shows the control effort and quadratic error. In this situation, considering γ_1 and γ_2 time variants, we obtained a more oscillatory result than the result obtained in case ”a”. But it still has a good performance, as the variation of γ_i causes a big change in the system (including the switch to non-minimum phase).

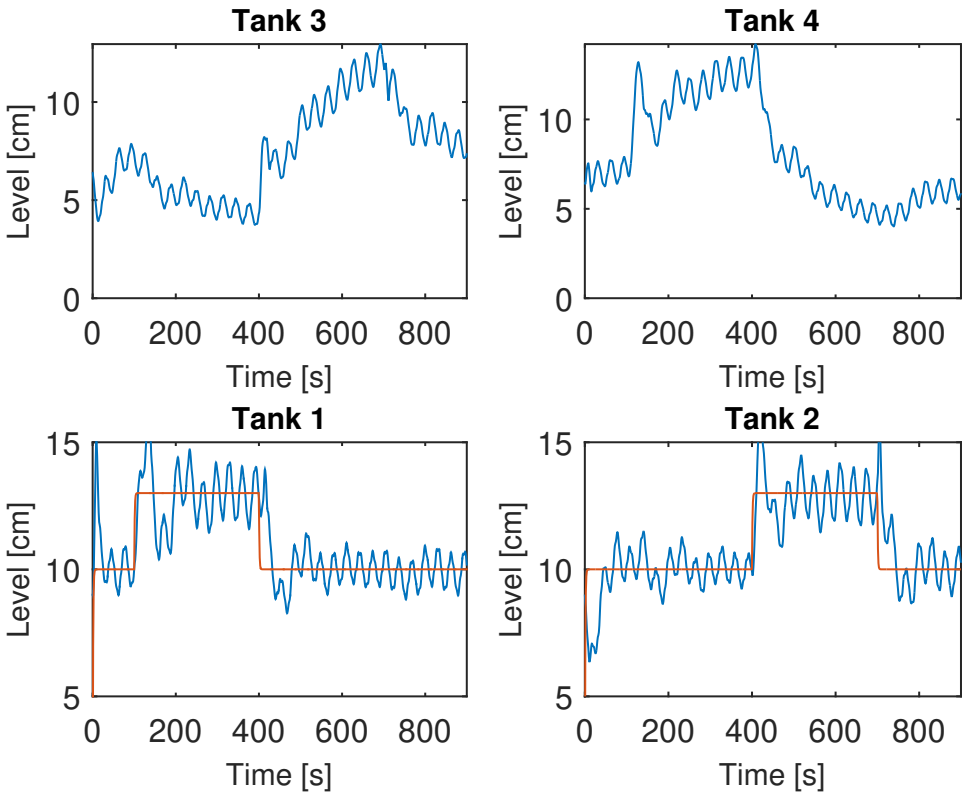

Figure 30: Outputs considering a step reference and γ_1 and γ_2 time variants.

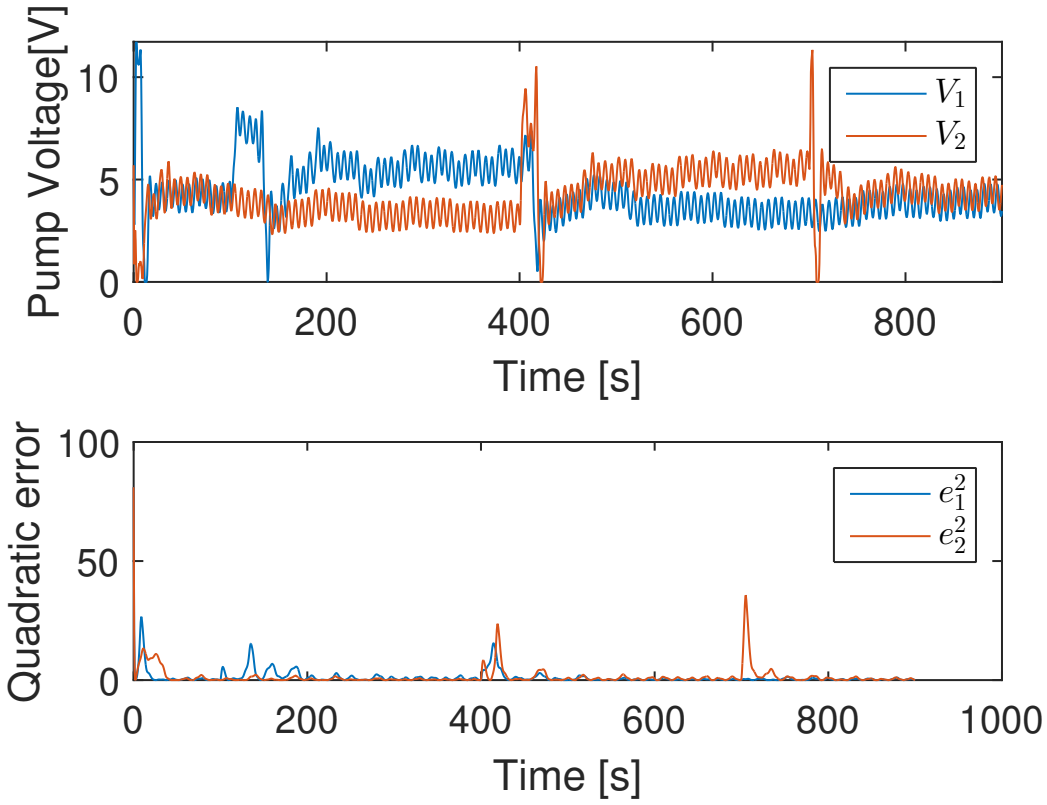

Figure 31: Control effort and quadratic error considering a step reference and γ_1 and γ_2 time variants.

5.4.4 Case d

Lastly, the case ”d” is the combination of case ”b” and case ”c”. The reference is the same considered in the case ”b”, but now with γ_1 and γ_2 time variants, as shown in Figure 29.

Figure 32 shows the output variables and 33 shows the control effort with quadratic error. The result obtained is similar to the case c and the output followed the reference but with a small oscillation around it.

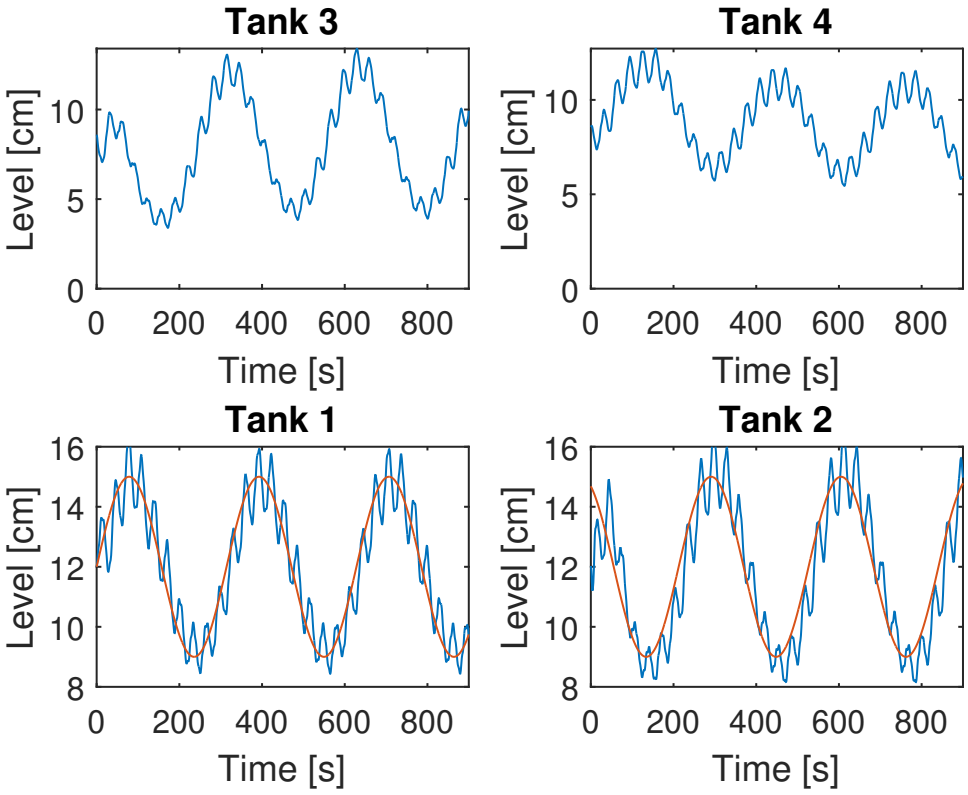

Figure 32: Outputs considering a sinusoidal reference and γ_1 and γ_2 time variants.

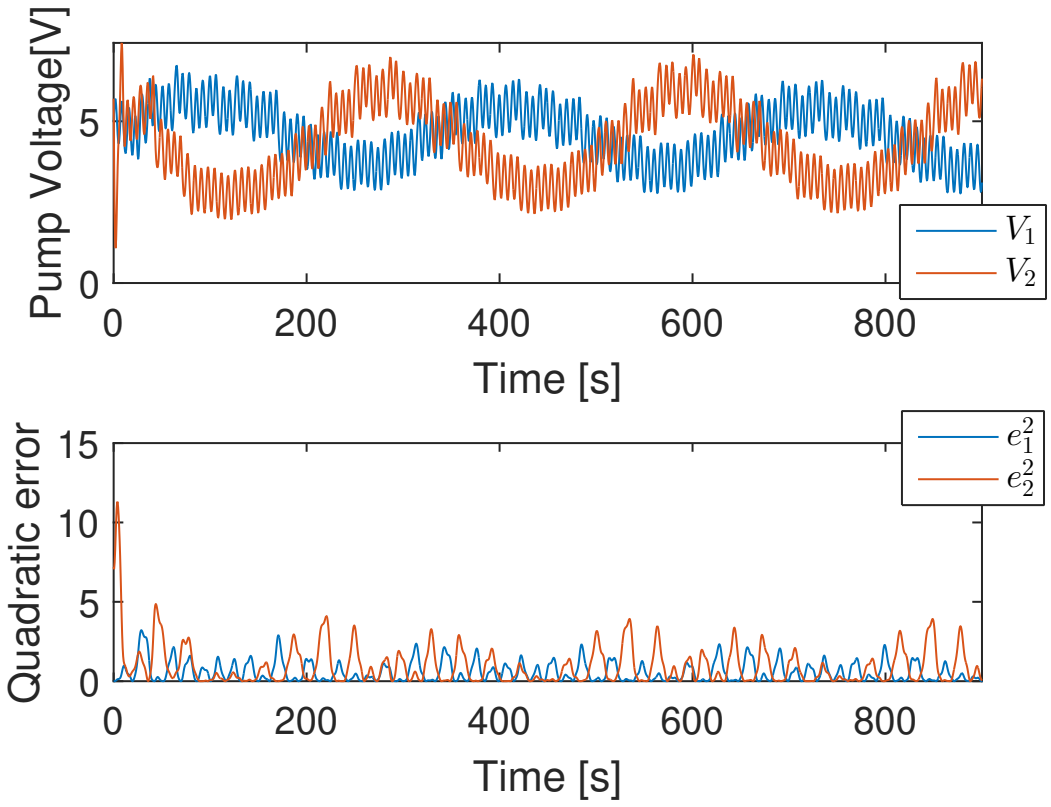

Figure 33: Control effort and quadratic error considering a sinusoidal reference and γ_1 and γ_2 time variants.

6 CONCLUSION

This work focuses on the study of identification of models and their implementation allied to predictive controllers. The study of predictive controller applied to the identified plant is part of it.

Firstly, the construction of the quadruple tank was explored and the phenomenological model was designed. This model is the basis for comparisons as it represents the quadruple tank mathematically. During the course of this work, as explored, the practical tank suffered some changes and because of that the scope of this work widened to include a model free control.

Then, the system identification was based on four different structures: ARX, ARMAX, OE and BJ. The four structures were tested in a forth order version to find which one has the best FIT with the phenomenological model. BJ structures presented the best FIT.

The MPC with finite horizon studied was presented and tested on this best-fit identified plant. The comparison this time was tested and validated with two reference tracking tests and a disturbance rejection test. The results were coherent solving stability and reference tracking problem. The same controller was tested between plants and as the results showed that adjustments were needed to have better outcomes.

The IHMPC was implemented using the OPOM model as base and, even though one of the outputs could be well controlled, the other one is not as good as the first. Another point is that the controller is too slow, almost a hundred times slower than the MPC. This shows that the application of this controller must take into account the type of plant that would be implemented, solving in a better manner the control problem for a slow plant.

Finally, an extremum-seeking control was used to solve a tracking problem in the plant. The presented ESC project does not consider the model of the system, this generates a model-free control technique. The control technique is composed of two decentralized ESC algorithms, where the first output is associated with the first input and the same

is done for the second output. To test the technique, some simulations were made using the nonlinear quadruple tank model. The results obtained were satisfactory, validating the model-free control technique. Furthermore, the performance was verified considering time-varying parameters.

In conclusion, the work tests two alternatives of control techniques in a model with low level of information of the plant. The identification uses only inputs and outputs and the second technique shows another way of creating a control to a plant in a situation were tests are not feasible.

As suggestions for future works, would be interesting to recreate the phenomenological model based on the new tank structure which would make possible the comparison between both models. Another point would be better tuning the controllers and testing them on the practical plant.

REFERENCES

AGUIRRE, L. *Introdução à Identificação de Sistemas – Técnicas Lineares e Não-Lineares Aplicadas a Sistemas Reais*. 4. ed. [S.l.]: Editora UFMG, 2015.

ARIYUR, K. et al. *Real-Time Optimization by Extremum-Seeking Control - Control Systems Magazine, IEEE*. [S.l.]: Editora Wiley-Interscience, 2003.

ASTROM, K.; JOHANSSON, K.; WANG, Q.-G. Design of decoupled pi controllers for two-by-two systems. *IEE Proceedings of Control Theory and Applications*, v. 149, n. 1, p. 74–81, Jan 2002.

DESTRO, R. et al. Direct extremum-seeking control applied to a quadruple tank system. In: . [S.l.: s.n.], 2021.

FERRAMOSCA, A. et al. Mpc for tracking target sets. In: *Proceedings of the 48h IEEE Conference on Decision and Control (CDC) held jointly with 2009 28th Chinese Control Conference*. [S.l.: s.n.], 2009. p. 8020–8025. ISSN 0191-2216.

JOHANSSON, K. The quadruple-tank process: a multivariable laboratory process with an adjustable zero. *IEEE Transactions on Control Systems Technology*, v. 8, n. 3, p. 456–465, May 2000.

KRSTIć, M.; WANG, H.-H. Stability of extremum seeking feedback for general nonlinear dynamic systems. *Automatica*, v. 36, n. 4, p. 595–601, 2000. ISSN 0005-1098.

LI, Z.; ZHENG, C. H_∞ loop shaping control for quadruple tank system. In: *Sixth International Conference on Intelligent Human-Machine Systems and Cybernetics (IHMSC)*. [S.l.: s.n.], 2014. v. 2, p. 117–120.

LJUNG, L. *System Identification: Theory for the User, Second Edition*. Englewood Cliffs, NJ: Prentice-Hall, 1999.

MARTINS M. A.; ODLOAK, D. A robustly stabilizing model predictive control strategy of stable and unstable processes. *Automatica*, v. 67, n. Supplement C, p. 132 – 143, 2016. ISSN 0005-1098.

NEVES, G. P. das; ANGÉLICO, B. A. Controle qft para o tanque quadruplo com desacoplamento dinâmico. In: *XXI Congresso Brasileiro de Automática - CBA2016*. [S.l.: s.n.], 2016. p. 374–378.

NEVES, G. P. das et al. Discrete time lqg/ltr applied to a practical quadruple tank system. In: *2016 IEEE Conference on Control Applications (CCA)*. [S.l.: s.n.], 2016. p. 1232–1237.

ODLOAK, D. Extended robust model predictive control. *AIChE Journal, American Institute of Chemical Engineers*, v. 50, n. 9, p. 1824 – 1836, 2004. ISSN 1547-5905.

QIN, S.; BADGWELL, T. A. A survey of industrial model predictive control technology. *Control Engineering Practice*, v. 11, n. 7, p. 733 – 764, 2003. ISSN 0967-0661. Disponível em: ⟨http://www.sciencedirect.com/science/article/pii/S0967066102001867⟩.

ZHANG, C.; ORDÓÑEZ, R. Extremum-seeking control and applications: A numerical optimization-based approach. In: . [S.l.]: Editora Springer, 2012.